Science of the Total Environment 959 (2025) 178260

Contents lists available at ScienceDirect

Science of the Total Environment

journal homepage: www.elsevier.com/locate/scitotenv

Degradation of organophosphate flame retardants by white-rot fungi: Degradation pathways and associated toxicity

Diana Losantos [a], Julio Fernández-Arribas [b], Míriam Pérez-Trujillo [c], Ethel Eljarrat [b], Montserrat Sarrà [a,*], Glòria Caminal [d]

[a] Department of Chemical, Biological and Environmental Engineering, Universitat Autònoma de Barcelona, Escola d'Enginyeria, Campus Bellaterra, 08193 Cerdanyola del Vallès, Spain
[b] Environmental and Water Chemistry for Human Health (ONHEALTH), Institute of Environmental Assessment and Water Research (IDAEA), Spanish Council for Scientific Research (CSIC), Jordi Girona 18-26, 08034 Barcelona, Spain
[c] Nuclear Magnetic Resonance Service, Universitat Autònoma de Barcelona, Campus Bellaterra, 08193 Cerdanyola del Vallès, Spain
[d] Institut de Química Avançada de Catalunya (IQAC), Spanish Council for Scientific Research (CSIC), Jordi Girona 18-26, 08034 Barcelona, Spain

HIGHLIGHTS

- Metabolites from the fungal degradation of TBP, TBEP, TCEP and TCPP were identified.
- OPFRs degraded mainly via hydroxylation, hydrolysis and oxidative dechlorination.
- Novel steps like dehydrogenation and reductive dechlorination were proposed.
- Microtox assays indicated increased toxicity after fungal degradation.
- ECOSAR predictions indicated potentially toxic products to be targeted.

GRAPHICAL ABSTRACT

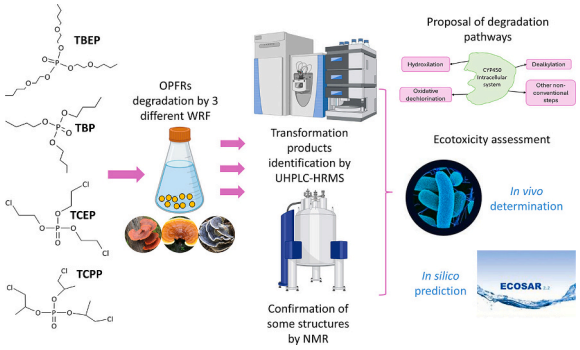

ARTICLE INFO

Editor: Damià Barceló

Keywords:
Biodegradation
OPFRs
Transformation products
Hydroxylation
Demethylation

ABSTRACT

The environmental persistence of organophosphate flame retardants (OPFRs) in water is becoming and environmental concern. White Rot Fungi (WRF) have proven its capability to degrade certain OPFRs such as tributyl phosphate (TBP), tris(2-butoxyethyl) phosphate (TBEP), tris(2-chloroethyl) phosphate (TCEP) and tris(2-chloroisopropyl) phosphate (TCPP). Despite this capability, there is limited knowledge about the specific pathways involved in the degradation. In this study, three different WRF were paired with individual OPFRs, and potential transformation products (TPs) were identified by UHPLC-HRMS. Some compounds structures were further validated by NMR. From these data degradation pathways were proposed. TBP was degraded by successive hydroxylation and hydrolysis reactions, with a novel dehydrogenation step suggested. Both TCEP and TCPP underwent oxidative dechlorination, with TCEP experiencing subsequent hydrolysis. Uncommon reductive dehalogenation was also observed. TCPP further underwent hydroxylation and environmentally relevant methylation. TBEP generated numerous TPs, mainly by successive dealkylations, along with hydroxylation. Notably, demethylation in TBEP degradation was proposed for the first time. Additional secondary products were

* Corresponding author.
E-mail address: montserrat.sarra@uab.cat (M. Sarrà).

https://doi.org/10.1016/j.scitotenv.2024.178260
Received 18 November 2024; Received in revised form 20 December 2024; Accepted 21 December 2024
Available online 2 January 2025

formed through hydroxylation and oxidation of the initial metabolites. Finally, in vivo and in silico toxicity assessments were conducted, identifying certain TPs as potentially toxic.

1. Introduction

Organophosphate flame retardants (OPFRs) have become widely used as fire inhibitors following the phasing out of polybrominated diphenyl ethers flame retardants from the European Union (Li et al., 2023; X. Zhang et al., 2023). These compounds are versatile additives found in various commercial products, including furniture wood, electronics, vehicles, plastics and textiles (Shi et al., 2016; S. Zhang et al., 2021). Some alkyl OPFRs have additional applications such as plasticizers and antifoaming agents (Kung et al., 2022). Several OPFRs are listed as high-production-volume chemicals (USEPA, 2023), with a global production estimated at 2.8 million tons in 2018 (Gustavsson et al., 2018).

Due to the large production and consumption of OPFRs, their environmental fate is drawing increasing attention. As additives, they usually lack chemical bonds with their base materials, leading to their release into various environmental matrices, including water compartments, throughout manufacturing, usage and disposal (Gbadamosi et al., 2023; Li et al., 2023). Domestic and industrial wastewater discharges are key sources of their gradual accumulation in water (Liang and Liu, 2016; Xu et al., 2019; Y. Zhang et al., 2023). Given their physicochemical properties, including moderate-to-high water solubility, five OPFRs: tri-n-butyl phosphate (TBP), tris (2-butoxy ethyl) phosphate (TBEP), tris(2-chloroethyl) phosphate (TCEP), tris(2-chloroisopropyl) phosphate (TCPP) and triethyl phosphate (TEP) are commonly found in wastewater treatment plants (WWTP) effluents (Lao et al., 2023; Petromelidou et al., 2024; Zhang et al., 2023), indicating that conventional treatment processes do not completely eliminate them.

This prevalence in water compartments has led to the accumulation of OPFRs in aquatic biota and humans. In the past five years, studies have detected these flame retardants in algae (Fu et al., 2020), invertebrates (Bekele et al., 2019; Castro et al., 2020; Choi et al., 2020; Wang et al., 2019; R. Zhang et al., 2020), fish (Bekele et al., 2021; Bekele et al., 2019; Choo et al., 2018; Garcia-Garin et al., 2020b; Liu et al., 2019c, 2019d; Wang et al., 2019) and higher trophic level organisms (Aznar-Alemany et al., 2019; Garcia-Garin et al., 2020a; Sala et al., 2019) across different water compartments. Their detection in arctic species (Fu et al., 2020), highlights their potential for long-range transport and bioaccumulation. Human exposure is evident through the presence of OPFRs in biological matrices such as urine, usually estimated via the produced metabolites (Chen et al., 2022; Guo et al., 2023; Li et al., 2024; Lu et al., 2022; Zhao et al., 2023), breast milk (Chen et al., 2021a, 2021b; Zhang et al., 2024; Zheng et al., 2021), saliva (Zhao et al., 2023), nails (Chen et al., 2019; Zhao et al., 2023), hair (Tang et al., 2021) and blood (Guo et al., 2023).

The widespread exposure has increased the number of studies focusing on the health risks associated with OPFRs. TBP is recognized for its neurotoxic effects (Chang et al., 2020), potential as an endocrine disruptor (Kojima et al., 2016; Zhang et al., 2017), and capability to impair reproductive health and cause DNA and cellular damage (Liu et al., 2019b; Ren et al., 2017; H. Zhang et al., 2021). Similarly, TBEP exposure has been linked to neurotoxicity (Jiang et al., 2018), endocrine disruption (Jin et al., 2016; Kwon et al., 2016; Ma et al., 2016; Q. Xu et al., 2017) and reproductive and developmental toxicity (Han et al., 2014; Huang et al., 2019; Kwon et al., 2016; Ma et al., 2016; Pan et al., 2022; Xiong et al., 2021; Q. Xu et al., 2017). TBEP also poses risks of hepatotoxicity and carcinogenicity (Ren et al., 2017; Saquib et al., 2022). TEP has shown potential neurotoxic and mutagenic effects at high doses (Lai et al., 2022) and it also acts as an endocrine disruptor, affecting embryonic development (Egloff et al., 2014). Both TCEP and TCPP are considered carcinogenic and neurotoxic (Li et al., 2019; National Toxicology Program, 2023; T. Xu et al., 2017). Moreover, TCPP showed genotoxic effects (Antonopoulou et al., 2022; Crump et al., 2012; Saquib et al., 2021) and lipid-metabolism disfunction related to its exposure (Yan et al., 2022), while TCEP can disrupt embryonic development, hormone levels, antioxidant enzymes activities and core receptors interactions (Chen et al., 2015; Hu et al., 2021; Sutha et al., 2022; Wang et al., 2022; Wu et al., 2017) and is potentially hepatotoxic (Al-Salem et al., 2020; Tian et al., 2023; Yang et al., 2022). In fact, due to its hazards, TCEP has been banned from childcare products in many U.S states and is regulated in the EU, along with TCPP, with a concentration limit of 5 mg/kg in toys for children under three years old (Negev et al., 2018).

Fungal bioremediation offers a promising, cost-effective, and eco-friendly approach for removing emergent contaminants, such as OPFRs, from wastewater. White-rot fungi (WRF) are particularly effective microorganisms widely studied because of their capability to constitutively degrade not only lignin and lignin-like substances, but also a series of xenobiotics, even at trace levels (Latif et al., 2023; Torres-Farradá et al., 2024). Although degradation has been mostly attributed to their extracellular enzymes, especially lignin-modifying enzymes with broad substrate specificity (Mir-Tutusaus et al., 2018; Zhuo and Fan, 2021), growing evidence indicates that the versatile intracellular CYP450 enzyme system of WRF also plays a crucial role in converting contaminants (Črešnar and Petrič, 2011; Durairaj et al., 2016).

The capability of WRF in degrading OPFRs has been previously substantiated in a screening study (Losantos et al., 2024b). Three fungi: *Trametes versicolor*, *Ganoderma lucidum* and *Pycnoporus sanguineus* were identified as potential candidates for future wastewater treatment in a co-culture approach. Each fungus was tested on a mixture of the five tested OPFRs. All three fungi successfully degraded TBEP completely. Similarly, TBP was fully eliminated after contact with *T. versicolor* and *G. lucidum,* but also effectively degraded by *P. sanguineus*. TCEP degradation was challenging, with only *G. lucidum* achieving partial degradation. The other chlorinated OPFR, TCPP, was more susceptible to degradation, with *T. versicolor* exhibiting the highest degradation efficiency, followed by *G. lucidum*, which degraded TCPP more effectively than TCEP. No substantial degradation of TEP was observed with any of the tested fungi. The results suggested that polarity of an OPFR inversely correlates with its susceptibility to fungal degradation.

Enzymatic system tests identified the intracellular CYP450 system as responsible for OPFRs degradation (Losantos et al., 2024b), suggesting that reactions of hydroxylation, dealkylation and dehalogenation might be involved in the degradation pathway. While the degradation pathway of TBP was already studied for *T. versicolor* (Tayar et al., 2024) and was found to be the same as for *G. lucidum*, the transformation products of TBP degradation by *P. sanguineus*, as well as those from other OPFRs, have yet to be determined. Furthermore, toxicity tests from the previous work, conducted on mixture solutions after fungal treatment with the three candidates, revealed that the obtained transformation products could be more toxic than the parent compounds, emphasizing the importance of identifying these products and assessing their individual toxicity.

In the present work, top fungal degraders were paired with their respective OPFR to identify the specific transformation products resulting from these degradations. As TEP was poorly degraded, it was excluded from this study. The transformation products were successfully identified and quantified by UHPLC-HRMS, while NMR analysis confirmed some of the structures, enabling us to propose degradation pathways. Toxicity was evaluated by a Microtox bioassay conducted at the beginning and end of each degradation experiment. Additionally, the individual toxicity of each transformation product was predicted by

means of the ECOlogical Structure Activity Relationships (ECOSAR) Class Program. To the best of our knowledge, this is the first comprehensive study that explores the degradation pathways of OPFRs by WRF and their possible environmental implications. By correlating the transformation products with their potential toxicity, this research helps to target potentially harmful compounds for future wastewater treatment strategies.

2. Materials and methods

2.1. Reagents

Standards of OPFRs were obtained from Merck KGaA (Darmstadt, Germany), including: tri-n-butyl phosphate (TBP ≥ 99 %), tris(2-butoxy ethyl) phosphate (TBEP 94 %), tris(2-chloroethyl) phosphate (TCEP 97 %) and a mixture of isomers (TCPP) containing 66.9 % of tris(1-chloro-2-propyl) phosphate (TCIPP/TCPP-IS1), 26.4 % of bis(1-chloro-2-propyl)(2-chloropropyl) phosphate (TCPP-IS2) and 4.2 % of (1-chloro-2-propyl) bis(2-chloropropyl) phosphate (TCPP-IS3). Stable isotopically labelled internal standards (IS) of isotopic purity ≥98 %: tri-n-butyl phosphate-d_{27} (dTnBP), tris[2-butoxy ($^{13}C_2$) ethyl] phosphate (M6TBEP) and tris(2-chloroethyl) phosphate-d_{12} (dTCEP) were purchased from Wellington laboratories (Guelph, Canada). High purity grade chemicals were used for culture media and analytical procedures.

2.2. Fungal strains and culture

The present study utilized three WRF: *Trametes versicolor, Ganoderma lucidum* and *Pycnoporus sanguineus*, chosen as the best candidates for OPFRs degradation (Losantos et al., 2024b). *Trametes versicolor* ATCC 42530 was obtained from the American Type Culture Collection (VA, USA), while *Ganoderma lucidum* FP-58537-Sp was acquired from the United States Department of Agriculture Collection (WI, USA). *Pycnoporus sanguineus* CS43 was gently supplied by the Environmental Bioprocesses Group of the Institute of Technology and Higher Studies of Monterrey (NL, México).

Strains were maintained by subculturing on malt extract agar plates at 25 °C every 30 days (Blánquez et al., 2008). The selected WRF were used in the form of pellets prepared in malt extract, according to a previously described methodology (Romero et al., 2006). Briefly, 1 mL of homogenised mycelial suspension was inoculated into 1000 mL Erlenmeyer flasks containing 250 mL of 2 % malt extract medium at a pH of 4.5. The flasks were incubated at 25 °C under continuous orbital agitation (135 rpm) for seven days. After incubation, the fungal biomass was separated from the medium and diluted in a 0.80 % (*w/v*) NaCl solution at a biomass/solution volumetric ratio of 1:1. The suspension was stored at 4 °C under sterile conditions until use.

2.3. Degradation experiments

Degradation experiments were conducted under conditions similar to those used in the previous screening study (Losantos et al., 2024b). The strain-OPFR combinations used in this study are presented in Table 1.

Fungal strains were maintained in 500 mL Erlenmeyer flasks containing 100 mL of sterile defined medium. The medium (pH = 4.5) contained per litre: 8 g glucose, 3.3 g ammonium tartrate, 1.168 g dimethyl succinate, 10 mL of a micronutrient's solution, and 100 mL of a macronutrient's solution from Kirk medium (Kirk et al., 1978). The compositions of each nutrient's solution are specified in Table S.1. Pellets of each tested fungus were initially inoculated at a concentration of ~3.5 g DCW·L^{-1} (DCW=Dry cell weight). The medium was enriched with each OPFR at the concentrations specified in Table 1, where the concentrations of the chlorinated OPFRs were half of the non-chlorinated ones, since they are more challenging to remove (Losantos et al., 2024b). The flasks were kept at 25 °C in the absence of light, under 135 rpm orbital shaking. On day 4, glucose was re-supplemented at a concentration of 3 g/L. After 15 days of degradation, the whole content of each flask was filtrated through glass microfiber filters (GF/A grade, ø = 47 mm; Whatmann™, Maidstone, UK) prior to transformation products (TPs) identification by UHPLC-HRMS and toxicity assessment. Samples were also analyzed by nuclear magnetic resonance (NMR) spectroscopy, which allowed to confirm some of the identified structures.

Table 1
Combinations of fungal candidate-OPFR used in the present study.

OPFR	Concentration at t_0 (ppm)	Fungal candidate
TCEP	5	*G. lucidum*
TBP	10	*P. sanguineus*
TBEP	10	*G. lucidum*
		P. sanguineus
TCPP	5	*G. lucidum*
		T. versicolor

2.4. Analytical procedures

2.4.1. Transformation products identification by UHPLC-HRMS

Immediately after completing the degradation experiments, 12 mL of the obtained filtrates (see section 2.3) were mixed with 50 μL of each IS corresponding to the initially transformed parent compound. For TCPP, dTCEP was used as the IS, being the most structurally similar to TCPP, out of the available ones. Afterwards, more filtrate was added until reaching a final volume of 25 mL. An aliquot was taken and filtered through 0.2 μm PTFE syringe filters (Interchim, Montluçon, France) prior to chromatographic analysis.

Identification of TPs was performed using an ultra-high-performance liquid chromatograph coupled to a hybrid quadrupole-Orbitrap mass spectrometer (UHPLC-Q-Exactive; Thermo Fisher Scientific, MA, USA). Chromatographic separation was achieved on a Purospher® STAR RP-18 end-capped Hibar® HR (150 × 2.1 mm, 2 μm) column (Merck KGaA). Acetonitrile (A) and ultrapure water containing 0.1 % formic acid (*v/v*) and 5 mM ammonium acetate (B) served as mobile phases. The mobile phases were fed at 0.2 mL/min in gradient mode. The elution program of A was changed as follows: 0 min, 20 %; 1 min, 20 %; 8 min, 95 %; 13 min, 95 %; 13.5 min, 20 %; and 15 min, 20 %. Sample injection volume was 10 μL.

Related to mass spectrometric conditions, an electrospray ionization (ESI) source was used in positive mode under a capillary voltage of 3000 V. The capillary and probe heater temperatures were set at 350 °C and 300 °C, respectively, while sheath and auxiliary gas flows were set at 40 and 10 arbitrary units.

Mass spectra were acquired in two consecutive scans. An initial full scan in the range 50–700 *m/z* was performed at a resolution of 70,000, followed by an MS/MS scan for all compounds reaching the analyzer, at a resolution of 35,000. The obtained data were processed using Compound Discoverer and Xcalibur software (Thermo Fisher Scientific). Potential TPs were identified based on molecular formula and mass accuracy (±5 ppm) of fragmented ions.

2.4.2. NMR analysis

Prior to instrumental analysis, sample cleanup was performed by Solid Phase Extraction (SPE) with Oasis HLB columns (30 mg; Waters Corporation, MA, USA), using a vacuum manifold connected to a vacuum pump. Filtrates from the degradation experiments (10 mL) were loaded onto columns priorly conditioned and equilibrated with 5 mL of methanol, and 5 mL of ultrapure water, respectively. The vacuum flow rate through the manifold was maintained at 5–10 mL·min^{-1}. After sample loading, the sorbent was washed with 5 mL of ultrapure water and dried under vacuum for 15 min. OPFRs were eluted by percolation with 8 mL of methanol. The eluate was dried under a gentle nitrogen

stream until complete evaporation of methanol. The dried samples were reconstituted in 600 μL of MeOD-d4 (99.80 % D, Cortecnet, Voisins-le-Bretonneux, France) and transferred to 5-mm-diameter NMR tubes.

A Bruker 400 Avance NEO NMR spectrometer (Bruker Biospin, Rheinstetten, Germany) operating at ^{1}H and ^{31}P NMR frequencies of 400.19 and 162.00 MHz, respectively, was used for the acquisition of standard 1D ^{31}P and ^{1}H decoupled ^{31}P ($^{31}P\{^{1}H\}$) NMR experiments and the 2D ^{1}H—^{31}P HMBC (Heteronuclear Multiple Bond Correlation) correlation. The spectrometer was equipped with a 5 mm iProbe 1H/BB/D with *Z*-gradients, and a BCU-II unit for temperature control. 1D spectra were acquired using standard 90° pulse sequences; in the case of $^{31}P\{^{1}H\}$, inverse-gated proton decoupling was utilized. In both cases, data were collected into 64 K data points during an acquisition time of 1.01 s and using a recycle delay of 1 s. Spectra were recorded in the time domain as interferograms (FID) across a spectral width of 32,680 Hz and as the sum of 1024 transients. FIDs were apodised applying an exponential function (0.2 Hz linebroadening) prior to Fourier transform (FT). Subsequently, the spectra were manually phased and baseline corrected. Phosphoric acid (85 %) in a glass capillary insert was used as external reference.

A Bruker Avance II 600 NMR spectrometer equipped with a 5 mm TBI probe with Z-gradients, operating at a ^{1}H and ^{13}C NMR frequencies of 600.13 and 150.90 MHz, respectively, and at 298.0 K of temperature, was used for the acquisition of 1D ^{1}H and 2D ^{1}H—^{1}H TOCSY (TOtal Correlation SpectroscopY) and multiplicity-edited ^{1}H—^{13}C HSQC (Heteronuclear Single Quantum Correlation) NMR experiments. 1D ^{1}H NMR spectra were acquired using a standard 90° pulse sequence, with an acquisition time of 1.51 s and a relaxation delay of 1 s. The data were collected into 32 K computer data points, with a spectral width of 10,822 Hz and as the sum of 1024 transients. The resulting free inductions decays (FIDs) were Fourier transformed, manually phased, and baseline corrected. The 2D NMR experiments were performed using standard pulse sequence (Bruker) and acquired under routine conditions. Unless otherwise stated, TMS (trimethylsilane) was used as external reference. The software TopSpin 3.6.3 (Bruker Biospin, Rheinstetten, Germany) was used to acquire, process and analyze the spectra.

In addition to the performance of 1D and 2D NMR spectra, ^{1}H and ^{13}C chemical shifts simulations were conducted using ChemDraw 22.2.0.

2.4.3. Toxicity assessment

2.4.3.1. Microtox test. Toxicity was measured for samples collected at the end of the degradation experiments and for parent compounds diluted in the defined medium at the initial concentrations chosen for each experiment (refer to Table 1). The pH of all samples was adjusted to 7 before testing, in accordance with the method. An acute toxicity bioassay kit (Modern Water, London, UK) was used, which measures the reduction in bioluminescence of marine *Vibrio fischeri* bacteria after 15-min exposure to specific sample dilutions. Toxicity was expressed in toxicity units (TU), calculated as shown in eq. 1.

$$TU = \frac{100}{EC50} \quad (1)$$

where EC50 is the concentration of the toxicant that inhibits 50 % of the bacteria at the end of the test.

2.4.3.2. Toxicity prediction. Since the Microtox test cannot determine the toxicity of each individual transformation product, theoretical toxicity was also predicted for these and the parent compounds. Predictions were made by means of the ECOlogical Structure Activity Relationships (ECOSAR) Class Program (v2.2: US Environmental Protection Agency, 2022). This computerized system estimates the acute (short-term) toxicity and chronic (long-term or delayed) toxicity of chemicals to aquatic organisms using Quantitative Structure Activity Relationships (SARs) and is employed by the US Environmental Protection Agency (EPA) for regulatory evaluations of aquatic toxicity.

Predictions included acute toxicity values such as LC50 (lethal concentration for 50 % of the population) for fish and daphnia after 96 and 48 h of exposure, respectively, and EC50 for green algae growth inhibition after 96 h of contact. These predictions were based on the molecular structure of each compound, entered into the software using either the CAS number or the SMILES code. Logarithm of the octanol-water partition coefficient (Log Kow) and water solubility were also provided by the program, as determined by the US EPA Estimation Programs Interface (EPI) Suite™.

3. Results and discussion

3.1. Identified TPs and proposed degradation pathways for each OPFR

The degradation experiments yielded the efficiencies represented in Table 2. These efficiencies were comparable to the previous work (Losantos et al., 2024b) and resulted in the detection of various TPs for each parent compound by UHPLC-HRMS. These findings led to the proposed degradation pathways presented below. Initially, triethyl phosphate (TEP) was suspected to be a common TP, as it was detected across all fungal matrixes. However, analysis of the initial samples revealed that TEP was present at the same concentrations as in the final samples, suggesting contamination of the starting compounds, perhaps originating from the synthesis process. This is plausible as TEP is commonly used as an intermediate in manufacturing (Kung et al., 2022). All parent compounds were fully characterized by ^{1}H, ^{13}C and ^{31}P NMR, while some products were also confirmed, as it will be further discussed in each subsection.

3.1.1. Degradation of TBP

Transformation products of TBP degradation were identified after fungal contact with the WRF *P. sanguineus*. Seven different metabolites were identified. These include three isomeric forms of dibutyl hydroxybutyl phosphate (TBP-M283/OH-TBP), two isomers of butyl bis-hydroxybutyl phosphate (TBP-M299/$(OH)_2$-TBP), dibutyl hydrogen phosphate (TBP-M211/DBP), two isomeric forms of butyl hydroxybutyl hydrogen phosphate (TBP-M227/OH-DBP) and two isomers of an unidentified compound designated as TBP-M265. Their chromatographic characteristics and respective areas are summarized in Table S.2.

The initial phase of the degradation pathway is likely hydroxylation, a primary detoxification mechanism recognized by eukaryotes and mammals CYP450 system for detoxifying contaminants (Črešnar and Petrič, 2011). In fact, the combined areas of the three isomers of OH-TBP indicate this product as the most abundant among the group, aligning with former proposed degradation pathways, where CYP-mediated hydroxylation was more important than hydrolysis to dialkyl phosphates (Hou et al., 2018; Sasaki et al., 1984).

NMR analysis evidenced hydroxylation of butyl moieties at the third

Table 2
Degradation efficiencies of the tested OPFRs after treatment with three different WRF. Analysis of the targeted OPFRs at the start and end of the experiment was conducted following the method of (Losantos et al., 2024a).

	Degradation efficiencies (%)		
Compound	*T.versicolor*	*G. lucidum*	*P. sanguineus*
TBP			59.54 ± 2.12
TBEP		100.00 ± 0.00	100.00 ± 0.00
TCEP		30.95 ± 1.04	
TCPP	76.70 ± 2.79	52.13 ± 5.33	

carbon position (Table S.3 and Fig. S.1 to S.3), matching with results from previous studies also regarding CYP450-mediated TBP degradation (Hou et al., 2018; Suzuki et al., 1984). Thus, it is highly likely that the most abundant TBP-M283 isomer (TBP-M283–1) corresponds to dibutyl 3-hydroxybutyl phosphate (3-OH-TBP). Further hydroxylation of 3-OH-TBP yields butyl bis(3-hydroxybutyl) phosphate (3,3-$(OH)_2$-TBP, corresponding to TBP-M299–1), which is subsequently hydrolyzed to 3-hydroxybutyl hydrogen phosphate (3-OH-DBP, designated as TBP-M227–1).

The presence of DBP (TBP-M211) was also confirmed by NMR (Table S.3 and Fig. S.1 to S.3) (Godinot et al., 2016). (Suzuki et al., 1984) demonstrated that DBP is generated through the oxidative hydrolysis of 3-OH-TBP, although direct cleavage of the ester bond in TBP is also possible (Liu et al., 2019a). Additionally, 3-OH-DBP (TBP-M227–1) might be also formed by hydroxylation of DBP, although this contribution appears to be minimal (Suzuki et al., 1984).

While the other isomers of OH-TBP could not be detected by NMR, probably related to their lower abundance, it is speculated that hydroxylation occurs at the second (2-OH-TBP/TBP-M283–2) and fourth carbon positions (4-OH-TBP/TBP-M283–3), as implied by (Suzuki et al., 1984). The detection of isomeric forms of both TBP-M299 and TBP-M227 suggests that one of the isomers of OH-TBP also undergoes these successive hydroxylation/hydrolysis steps. Prior conjectures indicate that the isomer performing these steps is 2-OH-TBP (Suzuki et al., 1984).

Finally, it is likely that TBP-M265 is formed through dehydrogenation of TBP. Although uncommon, CYP450-catalyzed dehydrogenation has been observed alongside hydroxylation (Erratico et al., 2015). In this scenario, unlike hydroxylation, the oxygen molecule is not introduced into the contaminant, but is entirely converted into two water molecules, resulting in an olefin (Wong et al., 2017). However, the position of the doble bond remains uncertain. It was proposed by (Reilly and Yost, 2005) that hydrogen is initially abstracted from the terminal carbon. Therefore, we theorize that the main isomer of TBP-M265 is a but-3-en-1-yl dibutyl phosphate. This compound's formation has solely been proposed in a study regarding triisobutyl phosphate (TiBP) transformation by an enriched activated sludge under aerobic conditions (Yao et al., 2023). We propose for the second isomer to contain the doble bond between the first and the second carbon atoms, although it could certainly be between the second and the third carbons.

The above discussion is depicted in Fig. 1. The proposed pathway closely resembles the one derived from TBP degradation by *T. versicolor* (Tayar et al., 2024) and *G. lucidum*, with some notable differences. Thus, $(OH)_2$-TBP isomers and TBP-M265 were not detected as transformation products, while monobutyl phosphate was produced by dealkylation of DBP only after 7 days of degradation (half the duration of this study). These differences not only underscore the different CYP450-mediated mechanisms between *P. sanguineus*, *T. versicolor* and *G. lucidum* in eliminating this contaminant, but also highlight the fact that degradation of DBP could pose a bottleneck in TBP degradation by *P. sanguineus*.

3.1.2. Degradation of TCEP

TCEP has demonstrated resistance against fungal degradation, resulting in only a small number of transformation products when in contact with *G. lucidum,* only fungal candidate of this work demonstrating efficiency in partially removing TCEP. In fact, scarce

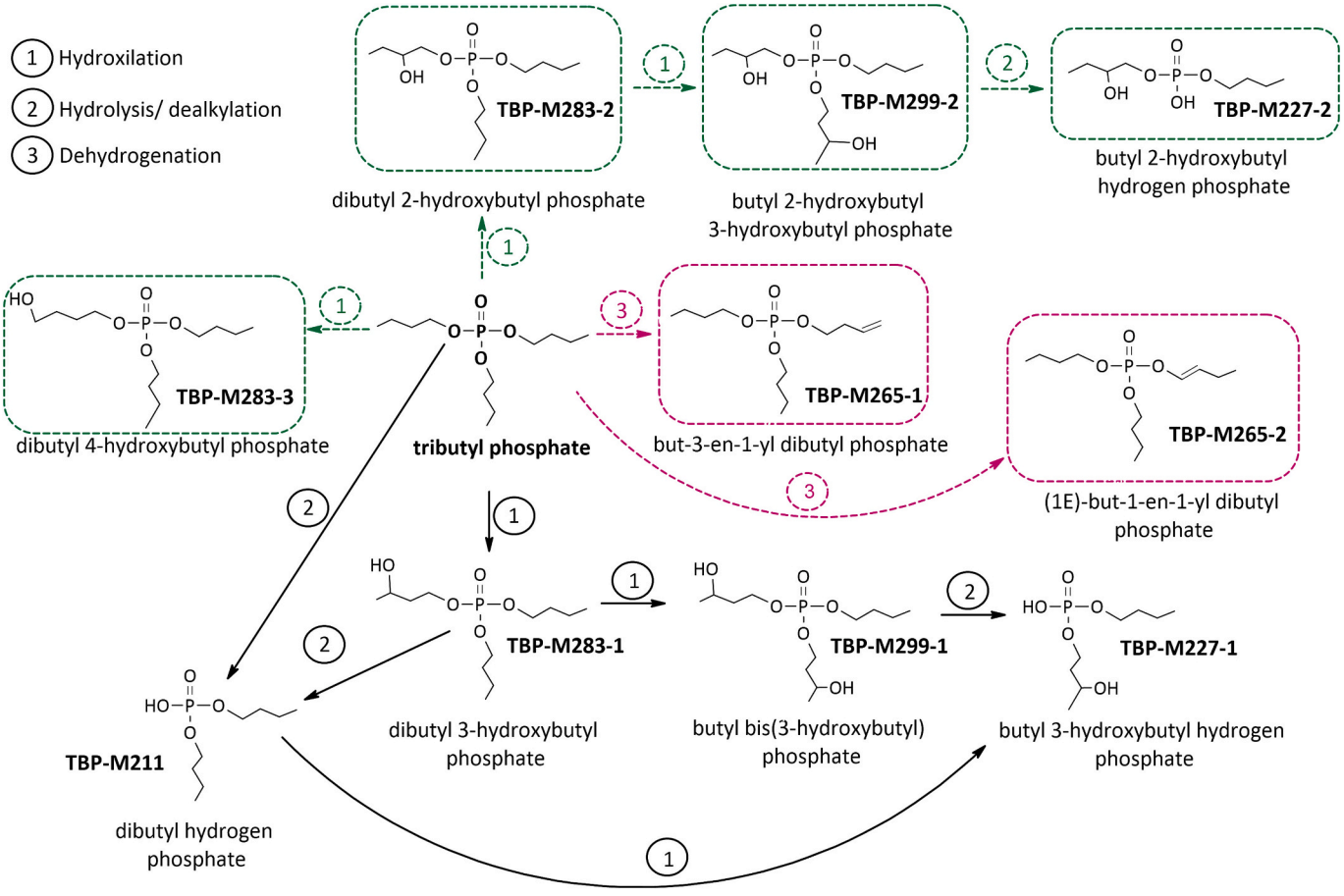

Fig. 1. Proposed metabolic pathway for TBP degradation by the fungus *P. sanguineus* after 15 days of experimentation. Solid lines denote degradative steps for compounds that are certain, while dashed lines indicate steps for the obtention of feasible compounds. The dehydrogenation step to produce TBP-M265 is highlighted in pink, representing a step proposed for the first time.

information about TCEP transformation products can be found in bibliography.

Table S.4 outlines four different transformation products that were obtained by UHPLC-HRMS: TCEP-M266, TCEP-M222, TCEP-M328 and TCEP-M231. The detection of bis(2-chloroethyl) 2-hydroxyethyl phosphate (BCEHEP/TCEP-M266) and the confirmation of the structure by NMR (Table S.5 and Figs. S.4 to S6), suggests that the first step in the degradation process is an oxidative dechlorination. This mechanism has been previously reported in the metabolism of TCEP by CYP450 enzymes in human liver preparations (Van den Eede et al., 2013). The reactivity of carbons linked to chlorine atoms likely explains this initial reaction (Wang et al., 2017).

The mass corresponding to TCEP-M222 matches that of bis(2-cloroethyl) hydrogen phosphate (BCEP). This product appeared at the same retention time as BCEHEP and could therefore be a fragment of this TP. In addition, BCEP could not be detected by NMR possibly due to its lower abundance. However, this diester has been identified as the main metabolite of TCEP degradation by numerous bibliographical sources (Federal Institute for Occupational Safety and Health, 2008; Hou et al., 2016; Takahashi et al., 2017), formed by the hydrolysis of BCEHEP (Hou et al., 2016). On the other hand, although TCEP-M328 was detected as the most abundant TP by UHPLC-HRMS, it was not observed by NMR. This molecule most likely represents an adduct formed in the ionization chamber of the UHPLC-MRS, resulting from the interaction between the theoretically unstable BCEHEP (Van den Eede et al., 2013) and chloroacetaldehyde, a by-product generated by the hydrolysis of BCEHEP to BCEP (Jia et al., 2022). This further supports the identification of BCEP as a transformation product. It also suggests that the abundance of BCEHEP might be underestimated, potentially making it the most prevalent compound. In certain cases, the hydrolysis of BCEP was reported as the bottleneck for complete mineralization of TCEP (Abe et al., 2017; Liang et al., 2022).

Finally, we theorize that TCEP-M231 is generated through the reductive dehalogenation of BCEHEP. Reductive dehalogenation involves the conversion of a C—Cl bond to a C—H bond (Van den Eede et al., 2013), which in this case would yield a double bond. While reductive dehalogenation under aerobic conditions is not commonly reported (Behrendorff, 2021), it has been suggested as a significant mechanism in the degradation of 2,4,6-trichlorophenol and pentachlorophenol by the WRF *Phanerochaete chrysosporium* (Reddy and Gold, 2000; Vijay et al., 1998). This aerobic dehalogenation most likely occurs via an intermediate conjugation between BCEHEP and the peptide glutathione (GSH), abundant in most cells (Couto et al., 2016; Reddy and Gold, 1999). Glutathione conjugation has been previously identified as a phase II reaction in the degradation of TCEP mediated by CYP450 glutathione S-transferases (Hou et al., 2016), which primarily targets chlorine substituents in the molecule (Testa and Krämer, 2010). Reduction of the resulting GS-conjugate is catalyzed by a reductase (Reddy and Gold, 2001). To the best of our knowledge, this is the first instance in which reductive dehalogenation mediated by the CYP450 system has been proposed for the degradation of OPFR. Further validation of this route should be performed, as the detection of TCEP-M231 by NMR was not possible due to the low concentration in the sample.

The proposed degradation pathway is depicted in Fig. 2.

3.1.3. Degradation of TCPP

The degradation of TCPP was assessed for a mixture of three isomers: tris(1-chloro-2-propyl) phosphate (TCIPP, 66.9 %), bis(1-chloro-2-

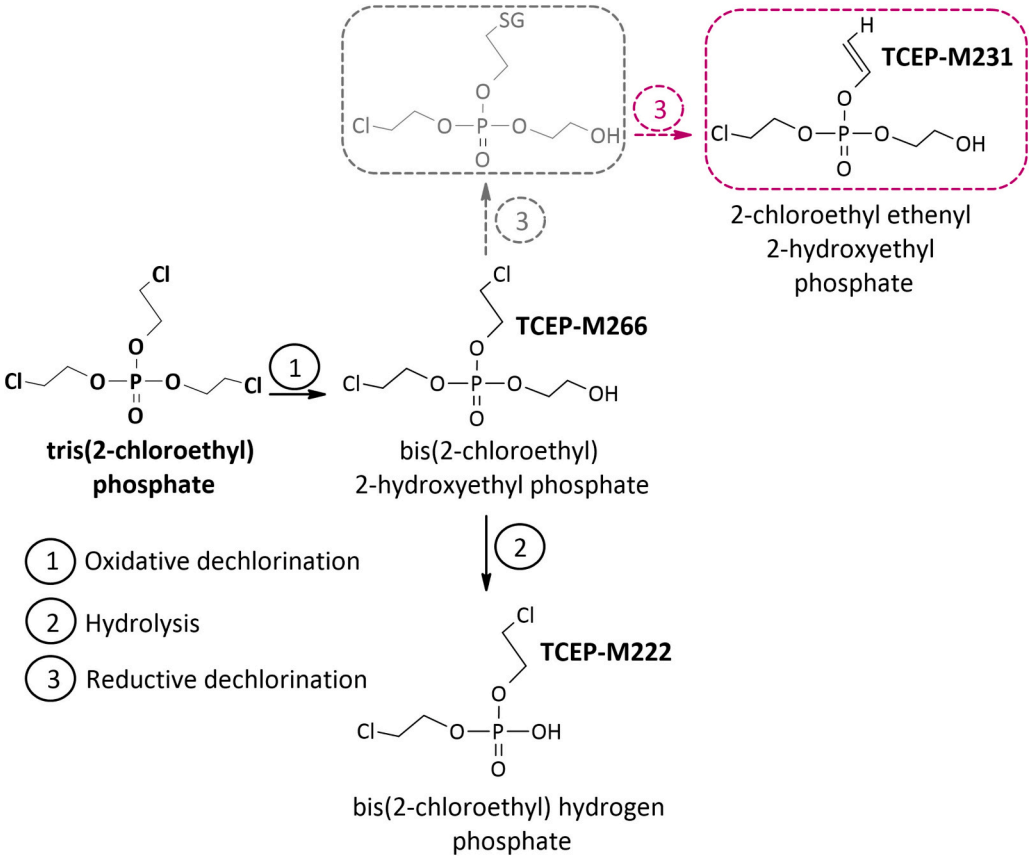

Fig. 2. Proposed metabolic pathway for TCEP degradation by the fungus *G. lucidum* after 15 days of experimentation. Solid lines denote degradative steps for compounds that are certain, while dashed lines indicate steps for the obtention of feasible compounds. The reductive dechlorination via GSH conjugation step to produce TCEP-M231 is highlighted in pink, representing a step proposed for the first time. The conjugated molecule between TCEP-M266 and GSH is represented in gray as the compound was not detected in the analyzed sample.

propyl)(2-chloropropyl) phosphate (TCPP-IS2, 26.4 %) and (1-chloro-2-propyl) bis(2-chloropropyl) phosphate (TCPP-IS3, 4.2 %). As displayed in Table S.6, five metabolites along with some isomeric forms were identified: TCPP-M309 (2 isomers), TCPP-M291, TCPP-M343 (2 isomers), TCPP-M323 and TCPP-M231. Quantification of these products was conducted following exposure to the two WRF demonstrating the most effective degrading performance, *Trametes versicolor* and *Ganoderma lucidum*. None of the identified TP's could be further confirmed by NMR analysis; therefore, the proposed degradation pathways are based solely on findings from literature.

Among these products, TCPP-M309/BCPHPP isomers were the most abundant, highlighting the relevance of oxidative dechlorination in the breakdown of chlorine-containing OPFRs, as previously observed in the case of TCEP. This finding also aligns with reported research (Abdallah et al., 2015; Van den Eede et al., 2016a), where BCPHPP was the main metabolite formed by mediation of the CYP450 system. The most abundant isomer likely belongs to TCIPP (BCIPHIPP) while the second isomer is attributed to the degradation of TCPP-IS2. The low concentration of TCPP-IS3 may have resulted in undetectable transformation products from its degradation.

Although analogous metabolites were anticipated for TCPP as for TCEP due to their structural resemblance, only BCPHPP shares similarity between these two. In the case of TCPP, a second oxidative dechlorination takes place, resulting in the formation of TCPP-M291/CPBHIPP, while in this case no reductive dechlorination metabolites were observed. On the other hand, hydroxylation of TCPP was evidenced by the presence of the TCPP-M343 (OH-TCPP) compound. Hydroxylation was also documented previously in TCPP degradation (Van den Eede et al., 2016b), although the detected compound had a low signal. In our study, OH-TCPP was the third most abundant metabolite, following BCPHPP and CPBHIPP. A second isomer of OH-TCPP, attributed to the degradation of TCPP-IS2 was only detected in samples exposed to *T. versicolor*. Although the position of the hydroxyl group is uncertain, it is likely that the CH_3 group is the primary binding site (Yu et al., 2019).

The presence of the product TCPP-M323 in both fungal matrixes suggest the methylation of BCPHPP. Methylation can occur as a CYP450 phase II metabolism step (Xiong et al., 2024), and has been reported as a major step in pentachlorophenol transformation by the WRF *Phanerochaete chrysosporium* (Ning and Wang, 2012). However, methylation might lead to an enhanced toxicity in nontarget organisms, due to increased hydrophobicity (Xiong et al., 2023), and so the environmental relevance of this compound should be assessed.

TCPP-M231 was exclusively detected in the sample after treatment with *G. lucidum*. It is likely that this compound is a tautomer of chloropropyl-hydroxypropyl phosphate. This suggests that *G. lucidum*, unlike *T. versicolor*, is capable of hydrolyzing at least one of the chains in the TCPP structure. Therefore, although common metabolites between the two tested fungi are more abundant with the treatment by *T. versicolor* while residual TCPP is lower, the extent of the degradation pathway is greater with *G. lucidum*, which is an important aspect to consider when evaluating fungal candidates.

Based on the preceding discussion, a degradation pathway was proposed for the main isomer of TCPP (TCIPP, see Fig. 3), assuming that all the main metabolites correspond to the degradation of this compound. Although it is not feasible to provide a detailed representation of the metabolic degradative reactions for the least abundant TCPP isomers, the presence of secondary isomers for BCPHPP and OH-TCPP implies that oxidative dechlorination and hydroxylation are the main steps in the degradation of these compounds.

3.1.4. Degradation of TBEP

The rapid depletion of TBEP, coupled with the ether bond within its structure, enabled the formation of 20 distinct transformation products, as detailed in Table S.7. These products were primarily identified for both *G. lucidum* and *P. sanguineus* (with the exception of TBEP-M285 in the case of the latter), suggesting a shared degradation pathway with

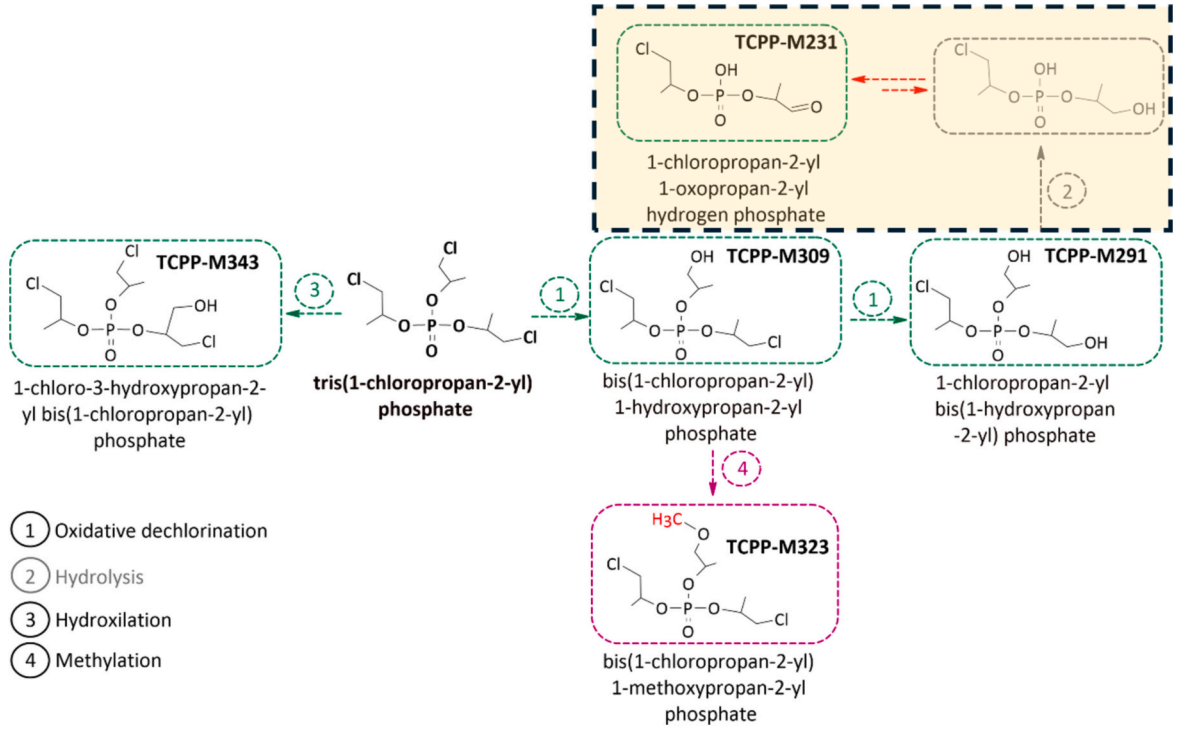

Fig. 3. Proposed metabolic pathway for TCPP (TCIPP) degradation by the fungi *G. lucidum* and *T. versicolor* after 15 days of experimentation. Solid lines denote degradative steps for compounds that are certain, while dashed lines indicate steps for the obtention of feasible compounds. Methylation to produce TCPP-M323 is highlighted in pink, representing a step proposed for the first time. TCPP-M231 is most likely a tautomer of the molecule in gray. The thermodynamic equilibrium displaced in this case to the ketonic form instead of the enolic form is represented by a longer red arrow. The area highlighted in orange represents a pathway that is only achieved by the fungus *G. lucidum*.

T. versicolor, the third fungal candidate also able to completely remove TBEP. The primary products were mainly produced by dealkylation of TBEP, although hydroxylation was also performed, along with demethylation, a step proposed for the first time in this study for TBEP degradation. Further secondary products were obtained by subsequent hydroxylation and oxidation reactions on the initially formed metabolites. For clarity, the degradation pathway was segmented into the obtention of the primary metabolites (refer to Fig. 4) and the subsequent hydroxylation and oxidation processes of each, detailed in figs. S.7-S11. Most of the primary metabolites were further confirmed by NMR, although none of the secondary metabolites were identified, except for one isomer of TBEP-M431, which will be discussed in greater detail.

TBEP-M415 was identified as the hydroxylated form of TBEP (OH-TBEP), proving that hydroxylation is an initial step in the metabolism of TBEP by the two tested fungi, as observed previously for the other tested OPFRs. For *P. sanguineus*, two isomers were detected, with the most abundant being 3-OH-TBEP (TBEP-M415–1), which was confirmed by NMR due to the observation of the presence of the 3-OH-butoxy moiety (Table S.8). This isomer was also identified as predominant in liver preparations through both NMR (Van den Eede et al., 2015) and comparison with authentic standards (Hou et al., 2018). The second isomer (TBEP-M415–2) is tentatively identified as 2-OH-TBEP, following the suggestions of (Van den Eede et al., 2015), consistent with the degradation pathway of TBP. In the case of *G. lucidum*, only one isomer of OH-TBEP was detected, most likely corresponding to 3-OH-TBEP. The occurrence of hydroxylation at the terminal carbon atoms of the butoxy moiety enhances the molecule's stability (Testa and Krämer, 2008).

Three secondary metabolites derived from OH-TBEP were identified and represented in Fig. S.7: TBEP-M413, TBEP-M431 and TBEP-M429. The detection of two isomers of TBEP-M431 ($(OH)_2$-TBEP) suggests further hydroxylation of the OH-TBEP isomers. Since NMR confirmed the presence of chains hydroxylated in the third carbon, one of these TPs could certainly be 3-$(OH)_2$-TBEP (TBEP-M431–1). We postulate that the other hydroxylation occurs either at the second carbon atom of 3-OH-TBEP (for both fungi), or at the third carbon atom of the proposed 2-OH-TBEP (for *P. sanguineus*).

Interestingly, two isomers were identified for TBEP-M413 in both *P. sanguineus* and *G. lucidum*, corresponding to the ketonic forms of OH-TBEP (Ket-OH-TBEP). This suggests that the second isomer of OH-TBEP may also be generated by *G. lucidum*, and probably completely transformed by the end of the experiment. TBEP-M429 (Ket-$(OH)_2$-TBEP) isomers could occur either through the hydroxylation of TBEP-M413 isomers or by the oxidation of one hydroxyl radical for each isomer of $(OH)_2$-TBEP.

TBEP-M343 was identified as bis(2-butoxyethyl) 2-hydroxyethyl phosphate (BBEHEP), through UHPLC-HRMS and was confirmed by NMR (Table S.8 and Figs. S.12 to S.14), given the detection of the 2-hydroxyethyl moiety bonded to a phosphorus group. The presence of this structure in the registered spectrum could also confirm the structure of TBEP-M287 (BEBHEP).

According to (Liang et al., 2023), BBEHEP results from the ether cleavage of OH-TBEP. TBEP-M341 is most likely the aldehyde form of BBEHEP (Ald-BBEHEP), obtained after oxidation. Additionally, two isomers of hydroxylated BBEHEP (TBEP-M359/OH-BBEHEP) were identified, suggesting hydroxylation of BBEHEP. The exact position of the hydroxyl group could not be confirmed by NMR probably due to a lower concentration in the sample, but it is possible that it occurs similarly to OH-TBEP hydroxylation, where the most abundant isomer (TBEP-M359–1) is hydroxylated at the third carbon, while the other (TBEP-M359–2) might be hydroxylated at the second carbon. The pair of hydroxylated aldehyde isomers (TBEP-M357/Ald-OH-BBEHEP), could result from either oxidation of OH-BBEHEP isomers, or hydroxylation of

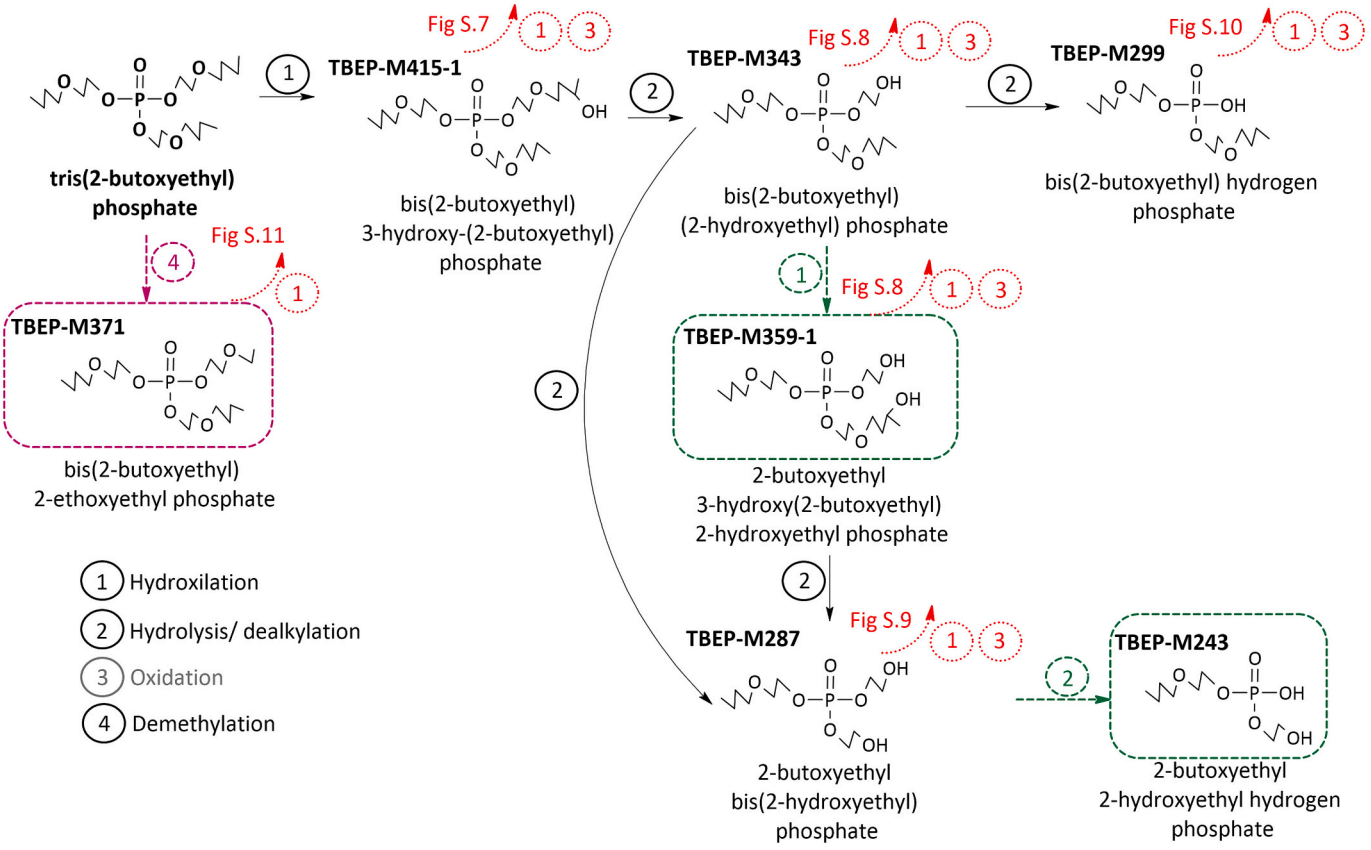

Fig. 4. Proposed metabolic pathway for TBEP degradation by the fungi *G. lucidum* and *P. sanguineus* after 15 days of experimentation. Solid lines denote degradative steps for compounds that are certain, while dashed lines indicate steps for the obtention of feasible compounds. Demethylation to produce TBEP-M371 is highlighted in pink, representing a step proposed for the first time.

Ald-BBEHEP, possibly at the third and second carbons, respectively. Finally, a subsequent hydroxylation of OH-BBEHEP isomers would yield the formation of two other isomers of TBEP-M375/$(OH)_2$-BBEHEP (refer to Fig. S.8).

TBEP-M287/BEBHEP could arise from dealkylation of either OH-BBEHEP (TBEP-M359) or BBEHEP (TBEP-M343). Additionally, we propose that TBEP-M303/OH-BEBHEP features the OH group on the third terminal carbon, like previously proposed hydroxylated metabolites. The aldehyde form of BEBHEP (TBEP-M285/Ald-BEBHEP) was only detected in *G. lucidum*, indicating that oxidation of this metabolite was not performed by *P. sanguineus*. The formation of these secondary metabolites is displayed in Fig. S.9. Furthermore, TBEP-M243/BEHEP can originate from hydrolysis of BEBHEP.

Further cleavage of the ethyl moiety in the reacting chain of BBEHEP could result in the formation of bis(2-butoxyethyl) hydrogen phosphate (TBEP-M299), also known as BBEP, the presence of which was confirmed by NMR (Table S.8 and Figs. S.12 to S.14) (Godinot et al., 2016). Two sequential hydroxylations (refer to Fig. S.10) would yield the formation of TBEP-M315/OH-BBEP (3 isomers, hypothesized to correspond to OH addition in the third, second, and first carbon of the butoxy moiety, respectively) and TBEP-M331/$(OH)_2$-BBEP (one isomer, possibly from hydroxylation of the first isomer of OH-BBEP at the third carbon).

An unknown transformation product, TBEP-M371 most likely corresponds to $C_{16}H_{35}O_7P$ (bis(2-butoxyethyl) 2-ethoxyethyl phosphate), although its identity was not verified by NMR. TBEP-M371 is possibly obtained by demethylation of the parent compound, where two methyl radicals are cleaved. Although this type of demethylation has been reported before for WRF (Grinhut et al., 2011; Hu et al., 2022), it is the first time it is reported as a step in TBEP degradation. Presumably, TBEP-M387 and TBEP-403 (two isomers) are obtained after successive hydroxilations of TBEP-M371 (see Fig. S.11). Addition of the OH group has been proposed to occur on the third carbon for TBEP-M387 and on the third and second carbon for the isomers of TBEP-403 following the trend used until now.

The numerous transformation products that were obtained make it challenging to determine the primary pathway, based on individual metabolite abundance, as most of the primary metabolites underwent further transformations, with varying extents between the fungal matrices. For practicality, areas were grouped into main transformation routes, where the primary products and their hydroxylated and oxidized derivatives were considered (refer to Table S.7).

The most important transformation route in both fungal matrices was TBEP initial hydrolysis to BBEHEP and its secondary products. These results align with other research, were BBEHEP (Liang et al., 2023; Van den Eede et al., 2015) and/or their secondary metabolites (Arukwe et al., 2018; Van den Eede et al., 2013) were the most abundant products. Hydroxylation and second hydrolysis also contribute significantly to TBEP transformation, although discrepancies were observed between the two tested fungi. Thus, hydroxylation products were more abundant than BEBHEP and its secondary metabolites for *G. lucidum*, whereas the opposite was true for *P. sanguineus*. Hydroxylation also proved relevant in TBEP degradation in liver preparations (Hou et al., 2018; Van den Eede et al., 2015) and wastewater treatment facilities (Choi and Kim, 2021).

Notably, BEBHEP was only recently detected for the first time as the second most abundant metabolite after bacterial degradation of TBEP (Liang et al., 2023), highlighting a newly reported pathway. The importance of the other degradation routes varies between fungal matrices. For instance, in the case of *P. sanguineus* the proposed demethylation route slightly outweighs hydrolysis to obtain BBEP, which in turn is the fourth most important route for *G. lucidum*. The formation of BEHEP cannot be comparable to the other proposed routes, as in this case no hydroxylated or oxidized secondary metabolites were detected.

3.2. Toxicity assessment

Toxicity data for the degradation of each parent compound to *Vibrio fischeri* is presented in Table 3. The results show a similar behavior to the toxicity observed in the degradation of compounds mixtures (Losantos et al., 2024b), where toxicity increases after degradation, confirming this pattern among all tested compounds. Additionally, the toxicity patterns align with findings from this previous study, where samples from the degradation with *P. sanguineus* exhibit the highest toxicity, followed by those with *T. versicolor*, and finally those with *G. lucidum*, which show the lowest toxicity.

Solubility in water, logarithm of the octanol-water partition coefficient (Log Kow), and theoretical LC50 and EC50 toxicity values for fish, daphnia and green algae were predicted by ECOSAR for each parent compound and the resulting TPs. These results are displayed in tables S.9-S.12. The generally lower Log Kow values indicate that all the surveyed metabolites are more hydrophilic than their parent compounds, with most of them also being more water-soluble (with a few exceptions that will be discussed). This suggests that most of the obtained TPs have a lower potential for bioaccumulation in aquatic organisms and humans (Hou et al., 2021) than their precursors.

In silico toxicity values were interpreted by comparison with the threshold values stablished by the Globally Harmonized System of Classification and Labelling of Chemicals (Winder et al., 2005). Thus, the compounds were classified into four categories regarding LC50 and EC50 values: very toxic (< 1 mg/L), toxic (between 1 and 10 mg/L), harmful (between 10 and 100 mg/L) and not harmful (>100 mg/L), with different colors representing each category, as explained in the supplementary section. Interestingly, all TPs displayed less toxicity than their parent compounds for the three reported organisms. This could suggest that the observed increase in toxicity after fungal degradation is caused by synergic effects of the mixtures of TPs.

By looking further into detail, there are some transformation products that despite having lower predicted toxicities, remain toxic or harmful to organisms reported in the ECOSAR, or have been reported to exhibit specific toxic traits. For instance, dehydrogenation of TBP, predicted to be toxic to all three organisms, results in TBP-M265 which remains toxic to daphnia, fish and green algae. OH-TBP, in its three isomeric forms, remains harmful for the tree organisms and is the most abundant TP. The presence of hydrophilic OH-functional groups can increase a compound's biological reactivity and potential toxicity (Choi and Kim, 2021). DBP, also potentially harmful for the reported organisms, has strong endocrine disrupting effects and may limit human nuclear receptor activity (Kojima et al., 2016; Q. Zhang et al., 2020). DBP is also commonly used as a biomarker for studying OPFRs effects in humans, along with other OPFRs diesters. As such, exposure to DBP has been associated with altered serum sex hormone levels in various age groups (Luo et al., 2020; Wei et al., 2020) and chronic kidney disease in humans (Kang et al., 2019). The presence of these numerous potentially toxics TPs could explain the elevated toxicity resulting from TBP degradation by *P. sanguineus*. Also, it is likely that samples degraded by *P. sanguineus* present a higher toxicity than those degraded by *T. versicolor* and *G. lucidum* because of the presence of TBP-M265 and the accumulation of DBP, although this should be verified.

In the case of TCEP, which is initially harmful to fish and green algae, none of the transformation products is harmful to the reported organisms. However, as explained before, it is likely that chloroacetaldehyde is an intermediate product in TCEP degradation pathway. Chloroacetaldehyde itself is predicted as harmful to fish (LC50 = 39.1 mg/L), daphnia (LC50 = 42.9 mg/L) and green algae (EC50 = 20.4 mg/L). Chloroacetaldehyde itself is predicted as harmful to fish (LC50 = 39.1 mg/L), daphnia (LC50 = 42.9 mg/L) and green algae (EC50 = 20.4 mg/L). On the other hand, although BCEP is predicted to be not harmful, human exposure to it has also been related to chronic kidney disease (Kang et al., 2019).

For TCPP, the higher abundance of transformation products after

Table 3
Toxicity of samples at the start and end of fungal degradation experiments for each parent compound.

	Toxicity units					
	TBP	TCEP	TCPP		TBEP	
	P. sanguineus	*G. lucidum*	*G. lucidum*	*T.versicolor*	*G. lucidum*	*P. sanguineus*
Initial	n.d	n.d	n.d	n.d	n.d	n.d
Final	7.72 ± 0.69	2.84 ± 0.11	2.32 ± 0.10	5.16 ± 0.04	3.89 ± 0.36	8.04 ± 0.36

degradation by *T. versicolor* compared to *G. lucidum*, which is associated with a greater degradation of TCPP (refer to Table 2), may explain the increased toxicity observed. Since TCPP is a mixture of three isomers, only the products from TCIPP degradation were analyzed using the ECOSAR program. TCIPP was predicted as harmful to all reported species, while TCIPP-M231 remained harmful for green algae. Considering that this product is exclusive to *G. lucidum* degradation, its contribution to overall toxicity may be less significant. TCIPP-M323 however, remains harmful to fish and green algae and is less water-soluble than TCIPP, indicating that methylation could increase toxicity. Lastly, OH-TCPP, continues to be harmful to fish and, similar to OH-TBP, could have potential toxicity. To the best of our knowledge, no specific toxic effects of any of the identified TPs for TCIPP degradation have been reported.

TBEP is harmful to fish and daphnia and toxic to green algae. Although most of the identified TPs are predicted to be non-harmful, some products might exert higher toxicity. This could be the case of the aldehydic form of BBEHEP (TBEP-M341) that remains harmful to all the species. Though BBEHEP and OH-TBEP are predicted as non-harmful, they are strong endocrine disruptors via nuclear receptors, unlike BBEP, which shows no activity (Kojima et al., 2016). For both fungal candidates (*P. sanguineus* and *G. lucidum*), hydrolysis for obtaining BBEHEP and its derivatives is the main degradation route, while hydroxylation is the second most important one for *P. sanguineus*. Another potentially toxic TP is TBEP-M371, harmful for all three reported species, indicating that demethylation is not an efficient route. These TPs were considerably more abundant in *P. sanguineus* than in *G. lucidum* (TP area ratio of 4.99 for BBEHEP and Ald-BBEHEP, 15.17 for OH-TBEP, and 24.65 for TBEP-M371), which could explain the notably higher toxicity observed after TBEP degradation by *P. sanguineus*, despite both fungi completely degrading TBEP and having a similar total abundance of TPs.

The experimental toxicities observed in *Vibrio fischeri* and the theoretical predicted values are valuable biological indicators of the potential harmful effects of the degradation of the tested OPFRs by WRF. However, since TPs were identified and toxicities were measured for each parent compound under controlled, sterile Erlenmeyer conditions, where even potentially toxic intermediate products (Ji et al., 2020; Van den Eede et al., 2016b) might accumulate without detection, these findings must be evaluated in the context of real wastewater treatment. In such environments, endogenous bacteria could further degrade the transformation products (Yang et al., 2020; Yu et al., 2019)potentially altering toxicity.

4. Conclusions

Transformation products were successfully identified for the fungal degradation of each targeted OPFR and pathways were proposed for the first time. Our findings highlight common mechanisms employed by the WRF for OPFRs degradation such as hydroxylation, hydrolysis and oxidative dechlorination. These mechanisms are consistent with the expected role of the CYP450 intracellular enzymatic system and are supported by previous studies that explored CYP450's role in OPFRs breakdown across various species.

Moreover, this study proposes novel degradation mechanisms such as dehydrogenation, reductive dechlorination, methylation and demethylation which have not been previously reported, adding new insights into OPFRs biological degradation. Additionally, several potentially toxic transformation products were identified, which will be prioritized for further evaluation in real wastewater experiments.

CRediT authorship contribution statement

Diana Losantos: Writing – original draft, Investigation, Formal analysis. **Julio Fernández-Arribas:** Investigation, Formal analysis. **Míriam Pérez-Trujillo:** Validation, Data curation. **Ethel Eljarrat:** Writing – review & editing, Supervision. **Montserrat Sarrà:** Writing – review & editing, Supervision, Funding acquisition, Conceptualization. **Glòria Caminal:** Writing – review & editing, Supervision, Methodology.

Funding

This work was supported by projects PID2019-103989RB-100 and TED2021-130639B-I00 financed by MCIN/AEI/10.13039/501100011033 and Unión Europea NextGenerationEU/PRTR. This work was partially supported by the Generalitat de Catalunya (Consolidated Research Group 2021-SGR-01008).

Diana Losantos acknowledges support from MCIN predoctoral research grant ref. PRE2020–095902.

Declaration of competing interest

The authors declare that they have no known competing financial interests or personal relationships that could have appeared to influence the work reported in this paper.

Appendix A. Supplementary data

Supplementary data to this article can be found online at https://doi.org/10.1016/j.scitotenv.2024.178260.

Data availability

Data will be made available on request.

References

Abdallah, M.A.E., Zhang, J., Pawar, G., Viant, M.R., Chipman, J.K., D'Silva, K., Bromirski, M., Harrad, S., 2015. High-resolution mass spectrometry provides novel insights into products of human metabolism of organophosphate and brominated flame retardants. Anal. Bioanal. Chem. 407, 1871–1883. https://doi.org/10.1007/s00216-015-8466-z.

Abe, K., Mukai, N., Morooka, Y., Makino, T., Oshima, K., Takahashi, S., Kera, Y., 2017. An atypical phosphodiesterase capable of degrading haloalkyl phosphate diesters from *Sphingobium* sp. strain TCM1. Sci. Rep. 7, 2842. https://doi.org/10.1038/s41598-017-03142-9.

Al-Salem, A.M., Saquib, Q., Al-Khedhairy, A.A., Siddiqui, M.A., Ahmad, J., 2020. Tris(2-chloroethyl) phosphate (TCEP) elicits hepatotoxicity by activating human cancer pathway genes in HepG2 cells. Toxics 8, 1–17. https://doi.org/10.3390/toxics8040109.

Antonopoulou, M., Vlastos, D., Dormousoglou, M., Bouras, S., Varela-Athanasatou, M., Bekakou, I.E., 2022. Genotoxic and toxic effects of the flame retardant tris (chloropropyl) phosphate (TCPP) in human lymphocytes. Microalgae and Bacteria. Toxics 10, 736. https://doi.org/10.3390/toxics10120736.

Arukwe, A., Carteny, C.C., Eggen, T., Möder, M., 2018. Novel aspects of uptake patterns, metabolite formation and toxicological responses in Salmon exposed to the

organophosphate esters—Tris(2-butoxyethyl)- and tris(2-chloroethyl) phosphate. Aquat. Toxicol. 196, 146–153. https://doi.org/10.1016/j.aquatox.2018.01.014.
Aznar-Alemany, Ò., Sala, B., Plön, S., Bouwman, H., Barceló, D., Eljarrat, E., 2019. Halogenated and organophosphorus flame retardants in cetaceans from the southwestern Indian Ocean. Chemosphere 226, 791–799. https://doi.org/10.1016/j.chemosphere.2019.03.165.
Behrendorff, J.B.Y.H., 2021. Reductive cytochrome P450 reactions and their potential role in bioremediation. Front. Microbiol. 12, 649273. https://doi.org/10.3389/fmicb.2021.649273.
Bekele, T.G., Zhao, H., Wang, Q., Chen, J., 2019. Bioaccumulation and trophic transfer of emerging organophosphate flame retardants in the marine food webs of Laizhou Bay, North China. Environ. Sci. Technol. 53, 13417–13426. https://doi.org/10.1021/acs.est.9b03687.
Bekele, T.G., Zhao, H., Wang, Q., 2021. Tissue distribution and bioaccumulation of organophosphate esters in wild marine fish from Laizhou Bay, North China: implications of human exposure via fish consumption. J. Hazard. Mater. 401, 123410. https://doi.org/10.1016/j.jhazmat.2020.123410.
Blánquez, P., Sarrà, M., Vicent, T., 2008. Development of a continuous process to adapt the textile wastewater treatment by fungi to industrial conditions. Process Biochem. 43, 1–7. https://doi.org/10.1016/j.procbio.2007.10.002.
Castro, V., Montes, R., Quintana, J.B., Rodil, R., Cela, R., 2020. Determination of 18 organophos- phorus flame retardants/plasticizers in mussel samples by matrix solid-phase dispersion combined to liquid chromatography-tandem mass spectrometry. Talanta 208, 120470. https://doi.org/10.1016/j.talanta.2019.120470.
Chang, Y., Cui, H., Jiang, X., Li, M., 2020. Comparative assessment of neurotoxicity impacts induced by alkyl tri-n-butyl phosphate and aromatic tricresyl phosphate in PC12 cells. Environ. Toxicol. 35, 1326–1333. https://doi.org/10.1002/tox.22997.
Chen, G., Jin, Y., Wu, Y., Liu, L., Fu, Z., 2015. Exposure of male mice to two kinds of organophosphate flame retardants (OPFRs) induced oxidative stress and endocrine disruption. Environ. Toxicol. Pharmacol. 40, 310–318. https://doi.org/10.1016/j.etap.2015.06.021.
Chen, Y., Cao, Z., Covaci, A., Li, C., Cui, X., 2019. Novel and legacy flame retardants in paired human fingernails and indoor dust samples. Environ. Int. 133, 105227. https://doi.org/10.1016/j.envint.2019.105227.
Chen, X., Li, W., Li, J., Fan, S., Shi, Z., 2021a. Rapid determination of 13 organophosphorus flame retardants in milk by using modified quick, easy, cheap, effective, rugged, and safe technique, solid-phase extraction, and HPLC-MS/MS. J. Sep. Sci. 44, 2269–2278. https://doi.org/10.1002/jssc.202001227.
Chen, X., Zhao, X., Shi, Z., 2021b. Organophosphorus flame retardants in breast milk from Beijing, China: occurrence, nursing infant's exposure and risk assessment. Sci. Total Environ. 771, 145404. https://doi.org/10.1016/j.scitotenv.2021.145404.
Chen, Z.F., Tang, Y.T., Liao, X.L., Jiang, J.R., Qi, Z., Cai, Z., 2022. A QuEChERS-based UPLC-MS/MS method for rapid determination of organophosphate flame retardants and their metabolites in human urine. Sci. Total Environ. 826, 153989. https://doi.org/10.1016/j.scitotenv.2022.153989.
Choi, Y., Kim, S.D., 2021. Identification and toxicity prediction of biotransformation molecules of organophosphate flame retardants by microbial reactions in a wastewater treatment plant. Int. J. Mol. Sci. 22, 5376. https://doi.org/10.3390/ijms22105376.
Choi, W., Lee, S., Lee, H.K., Moon, H.B., 2020. Organophosphate flame retardants and plasticizers in sediment and bivalves along the Korean coast: occurrence, geographical distribution, and a potential for bioaccumulation. Mar. Pollut. Bull. 156, 11275. https://doi.org/10.1016/j.marpolbul.2020.111275.
Choo, G., Cho, H.S., Park, K., Lee, J.W., Kim, P., Oh, J.E., 2018. Tissue-specific distribution and bio- accumulation potential of organophosphate flame retardants in crucian carp. Environ. Pollut. 239, 161–168. https://doi.org/10.1016/j.envpol.2018.03.104.
Couto, N., Wood, J., Barber, J., 2016. The role of glutathione reductase and related enzymes on cellular redox homoeostasis network. Free Radic. Biol. Med. 95, 27–42. https://doi.org/10.1016/j.freeradbiomed.2016.02.028.
Črešnar, B., Petrič, Š., 2011. Cytochrome P450 enzymes in the fungal kingdom. Biochim. Biophys. Acta, Proteins Proteomics 1814, 29–35. https://doi.org/10.1016/j.bbapap.2010.06.020.
Crump, D., Chiu, S., Kennedy, S.W., 2012. Effects of tris(1,3-dichloro-2-propyl) phosphate and tris(1-chloropropyl) phosphate on cytotoxicity and mRNA expression in primary cultures of avian hepatocytes and neuronal cells. Toxicol. Sci. 126, 140–148. https://doi.org/10.1093/toxsci/kfs015.
Durairaj, P., Hur, J.S., Yun, H., 2016. Versatile biocatalysis of fungal cytochrome P450 monooxygenases. Microb. Cell Factories 15, 1–16. https://doi.org/10.1186/s12934-016-0523-6.
Egloff, C., Crump, D., Porter, E., Williams, K.L., Letcher, R.J., Gauthier, L.T., Kennedy, S. W., 2014. Tris(2-butoxyethyl) phosphate and triethyl phosphate alter embryonic development, hepatic mRNA expression, thyroid hormone levels, and circulating bile acid concentrations in chicken embryos. Toxicol. Appl. Pharmacol. 279, 303–310. https://doi.org/10.1016/j.taap.2014.06.024.
Erratico, C.A., Deo, A.K., Bandiera, S.M., 2015. Regioselective versatility of monooxygenase reactions catalyzed by CYP2B6 and CYP3A4: examples with single substrates. In: Hrycay, E.G., Bandiera, S.M. (Eds.), Monooxygenase, Peroxidase and Peroxygenase Properties and Mechanisms of Cytochrome P450. Springer, pp. 131–149.
Federal Institute for Occupational Safety and Health, 2008. Tris (2-Chloroethyl) Phosphate, TCEP. Summary Risk Assessment Report.
Fu, Jie, Fu, K., Gao, K., Li, H., Xue, Q., Chen, Y., Wang, L., Shi, J., Fu, Jianjie, Zhang, Q., Zhang, A., Jiang, G., 2020. Occurrence and trophic magnification of organophosphate esters in an Antarctic ecosystem: insights into the shift from legacy to emerging pollutants. J. Hazard. Mater. 396, 122742. https://doi.org/10.1016/j.jhazmat.2020.122742.
Garcia-Garin, O., Sala, B., Aguilar, A., Vighi, M., Víkingsson, G.A., Chosson, V., Eljarrat, E., Borrell, A., 2020a. Organophosphate contaminants in North Atlantic fin whales. Sci. Total Environ. 721, 137768. https://doi.org/10.1016/j.scitotenv.2020.137768.
Garcia-Garin, O., Vighi, M., Sala, B., Aguilar, A., Tsangaris, C., Digka, N., Kaberi, H., Eljarrat, E., Borrell, A., 2020b. Assessment of organophosphate flame retardants in Mediterranean *Boops boops* and their relationship to anthropization levels and microplastic ingestion. Chemosphere 252, 126569. https://doi.org/10.1016/j.chemosphere.2020.126569.
Gbadamosi, M.R., Al-Omran, L.S., Abdallah, M.A.E., Harrad, S., 2023. Concentrations of organophos- phate esters in drinking water from the United Kingdom: implications for human exposure. Emerg Contam 9, 100203. https://doi.org/10.1016/j.emcon.2023.100203.
Godinot, C., Gaysinski, M., Thomas, O.P., Ferrier-Pagès, C., Grover, R., 2016. On the use of ^{31}P NMR for the quantification of hydrosoluble phosphorus-containing compounds in coral host tissues and cultured zooxanthellae. Sci. Rep. 6, 21760. https://doi.org/10.1038/srep21760.
Grinhut, T., Hertkorn, N., Schmitt-Kopplin, P., Hadar, Y., Chen, Y., 2011. Mechanisms of humic acids degradation by white rot fungi explored using ^{1}H NMR spectroscopy and FTICR mass spectro- metry. Environ. Sci. Technol. 45, 2748–2754. https://doi.org/10.1021/es1036139.
Guo, Y., Chen, M., Liao, M., Su, S., Sun, W., Gan, Z., 2023. Organophosphorus flame retardants and their metabolites in paired human blood and urine. Ecotoxicol. Environ. Saf. 268, 115696. https://doi.org/10.1016/j.ecoenv.2023.115696.
Gustavsson, J., Wiberg, K., Ribeli, E., Nguyen, M.A., Josefsson, S., Ahrens, L., 2018. Screening of organic flame retardants in Swedish river water. Sci. Total Environ. 625, 1046–1055. https://doi.org/10.1016/j.scitotenv.2017.12.281.
Han, Z., Wang, Q., Fu, J., Chen, H., Zhao, Y., Zhou, B., Gong, Z., Wei, S., Li, J., Liu, H., Zhang, X., Liu, C., Yu, H., 2014. Multiple bio-analytical methods to reveal possible molecular mechanisms of developmental toxicity in zebrafish embryos/larvae exposed to tris(2-butoxyethyl) phosphate. Aquat. Toxicol. 150, 175–181. https://doi.org/10.1016/j.aquatox.2014.03.013.
Hou, R., Xu, Y., Wang, Z., 2016. Review of OPFRs in animals and humans: absorption, bioaccumu- lation, metabolism, and internal exposure research. Chemosphere 153, 78–90. https://doi.org/10.1016/j.chemosphere.2016.03.003.
Hou, R., Huang, C., Rao, K., Xu, Y., Wang, Z., 2018. Characterized in vitro metabolism kinetics of alkyl organophosphate esters in fish liver and intestinal microsomes. Environ. Sci. Technol. 52, 3202–3210. https://doi.org/10.1021/acs.est.7b05825.
Hou, R., Wang, Y., Zhou, S., Zhou, L., Yuan, Y., Xu, Y., 2021. Aerobic degradation of nonhalogenated organophosphate flame esters (OPEs) by enriched cultures from sludge: kinetics, pathways, bacterial community evolution, and toxicity evaluation. Sci. Total Environ. 760, 143385. https://doi.org/10.1016/j.scitotenv.2020.143385.
Hu, F., Zhao, Y., Yuan, Y., Yin, L., Dong, F., Zhang, W., Chen, X., 2021. Effects of environmentally relevant concentrations of tris (2-chloroethyl) phosphate (TCEP) on early life stages of zebrafish (*Danio rerio*). Environ. Toxicol. Pharmacol. 83, 103600. https://doi.org/10.1016/j.etap.2021.103600.
Hu, K., Barbieri, M.V., López-García, E., Postigo, C., López De Alda, M., Caminal, G., Sarrà, M., 2022. Fungal degradation of selected medium to highly polar pesticides by *Trametes versicolor*: kinetics, biodegradation pathways, and ecotoxicity of treated waters. Anal. Bioanal. Chem. 414, 439–449. https://doi.org/10.1007/s00216-021-03267-x/Published.
Huang, Y., Liu, J., Yu, L., Liu, C., Wang, J., 2019. Gonadal impairment and parental transfer of tris (2-butoxyethyl) phosphate in zebrafish after long-term exposure to environmentally relevant concentrations. Chemosphere 218, 449–457. https://doi.org/10.1016/j.chemosphere.2018.11.139.
Ji, Q., He, H., Gao, Z., Wang, X., Yang, S., Sun, C., Li, S., Wang, Y., Zhang, L., 2020. UV/H_2O_2 oxidation of tri(2-chloroethyl) phosphate: intermediate products, degradation pathway and toxicity evaluation. J. Environ. Sci. (China) 98, 55–61. https://doi.org/10.1016/j.jes.2020.05.015.
Jia, Y., Yao, T., Ma, G., Xu, Q., Zhao, X., Ding, H., Wei, X., Yu, H., Wang, Z., 2022. Computational insight into biotransformation profiles of organophosphorus flame retardants to their diester metabolites by cytochrome P450. Molecules 27, 2799. https://doi.org/10.3390/molecules27092799.
Jiang, F., Liu, J., Zeng, X., Yu, L., Liu, C., Wang, J., 2018. Tris (2-butoxyethyl) phosphate affects motor behavior and axonal growth in zebrafish (*Danio rerio*) larvae. Aquat. Toxicol. 198, 215–223. https://doi.org/10.1016/j.aquatox.2018.03.012.
Jin, Y., Chen, G., Fu, Z., 2016. Effects of TBEP on the induction of oxidative stress and endocrine disruption in Tm3 Leydig cells. Environ. Toxicol. 31, 1276–1286. https://doi.org/10.1002/tox.22137.
Kang, H., Lee, J., Lee, J.P., Choi, K., 2019. Urinary metabolites of organophosphate esters (OPEs) are associated with chronic kidney disease in the general US population, NHANES 2013–2014. Environ. Int. 131, 105034. https://doi.org/10.1016/j.envint.2019.105034.
Kirk, T.K., Schultz, E., Connors, W.J., Lorenz, L.F., Zeikus, J.G., 1978. Influence of culture parameters on lignin metabolism by *Phanerochaete chrysosporium*. Arch. Microbiol. 117, 277–285. https://doi.org/10.1007/BF00738547.
Kojima, H., Takeuchi, S., Van den Eede, N., Covaci, A., 2016. Effects of primary metabolites of organophosphate flame retardants on transcriptional activity via human nuclear receptors. Toxicol. Lett. 245, 31–39. https://doi.org/10.1016/j.toxlet.2016.01.004.
Kung, H.C., Hsieh, Y.K., Huang, B.W., Cheruiyot, N.K., Chang-Chien, G.P., 2022. An overview: organophosphate flame retardants in the atmosphere. Aerosol Air Qual. Res. 22, 220148. https://doi.org/10.4209/aaqr.220148.

Kwon, B., Shin, H., Moon, H.B., Ji, K., Kim, K.T., 2016. Effects of tris(2-butoxyethyl) phosphate exposure on endocrine systems and reproduction of zebrafish (*Danio rerio*). Environ. Pollut. 214, 568–574. https://doi.org/10.1016/j.envpol.2016.04.049.

Lai, Y.J., Wang, X.W., Liu, J.F., 2022. Occurrence of trimethyl phosphate and triethyl phosphate in a municipal wastewater treatment plant and human urine. Environmental Pollutants and Bioavailability 34, 146–153. https://doi.org/10.1080/26395940.2022.2064338.

Lao, J.Y., Xu, S., Zhang, K., Lin, H., Cao, Y., Wu, R., Tao, D., Ruan, Y., Yee Leung, K.M., Lam, P.K.S., 2023. New perspective to understand and prioritize the ecological impacts of organophos- phate esters and transformation products in urban stormwater and sewage effluents. Environ. Sci. Technol. 57, 11656–11665. https://doi.org/10.1021/acs.est.3c04159.

Latif, W., Ciniglia, C., Iovinella, M., Shafiq, M., Papa, S., 2023. Role of white rot fungi in industrial wastewater treatment: a review. Applied Sciences (Switzerland) 13, 8318. https://doi.org/10.3390/app13148318.

Li, R., Wang, H., Mi, C., Feng, C., Zhang, L., Yang, L., Zhou, B., 2019. The adverse effect of TCIPP and TCEP on neurodevelopment of zebrafish embryos/larvae. Chemosphere 220, 811–817. https://doi.org/10.1016/j.chemosphere.2018.12.198.

Li, W., Yuan, Y., Wang, S., Liu, X., 2023. Occurrence, spatiotemporal variation, and ecological risks of organophosphate esters in the water and sediment of the middle and lower streams of the Yellow River and its important tributaries. J. Hazard. Mater. 443, 130153. https://doi.org/10.1016/j.jhazmat. 2022.130153.

Li, Y., Dai, Y., Luo, X., Zhang, L., Yuan, J., Tan, L., 2024. Biomonitoring urinary organophosphorus flame retardant metabolites by liquid–liquid extraction and ultra-high performance liquid chromatography-tandem mass spectrometry and their association with oxidative stress. Anal. Bioanal. Chem. 416, 4543–4554. https://doi.org/10.1007/s00216-024-05393-8.

Liang, K., Liu, J., 2016. Understanding the distribution, degradation and fate of organophosphate esters in an advanced municipal sewage treatment plant based on mass flow and mass balance analysis. Sci. Total Environ. 544, 262–270. https://doi.org/10.1016/J.SCITOTENV.2015.11.112.

Liang, Y., Zhou, X., Wu, Yiding, Wu, Yang, Gao, S., Zeng, X., Yu, Z., 2022. Rhizobiales as the key member in the synergistic Tris (2-chloroethyl) phosphate (TCEP) degradation by two bacterial consortia. Water Res. 218, 118464. https://doi.org/10.1016/j.watres.2022.118464.

Liang, Y., Zhou, X., Wu, Yiding, Wu, Yang, Zeng, X., Yu, Z., Peng, P., 2023. Meta-omics elucidates key degraders in a bacterial tris(2-butoxyethyl) phosphate (TBOEP)-degrading enrichment culture. Water Res. 233, 119774. https://doi.org/10.1016/j.watres.2023.119774.

Liu, J., Lin, H., Dong, Y., Li, B., 2019a. Elucidating the biodegradation mechanism of tributyl phosphate (TBP) by *Sphingomonas* sp. isolated from TBP-contaminated mine tailings. Environ. Pollut. 250, 284–291. https://doi.org/10.1016/j.envpol.2019.03.127.

Liu, Q., Tang, X., Wang, Y., Yang, Y., Zhang, W., Zhao, Y., Zhang, X., 2019b. ROS changes are responsible for tributyl phosphate (TBP)-induced toxicity in the alga *Phaeodactylum tricornutum*. Aquat. Toxicol. 208, 168–178. https://doi.org/10.1016/j.aquatox.2019.01.012.

Liu, Y.E., Luo, X.J., Huang, L.Q., Zeng, Y.H., Mai, B.X., 2019c. Organophosphorus flame retardants in fish from Rivers in the Pearl River Delta, South China. Sci. Total Environ. 663, 125–132. https://doi.org/10.1016/j.scitotenv.2019.01.344.

Liu, Y.E., Luo, X.J., Zapata Corella, P., Zeng, Y.H., Mai, B.X., 2019d. Organophosphorus flame retardants in a typical freshwater food web: bioaccumulation factors, tissue distribution, and trophic transfer. Environ. Pollut. 255, 113286. https://doi.org/10.1016/j.envpol.2019.113286.

Losantos, D., Palacios, O., Berge, M.J., Sarrà, M., Caminal, G., Eustaquio, A., 2024a. Novel method for rapid monitoring of OPFRs by LLE and GC–MS as a tool for assessing biodegradation: validation and applicability. Anal. Bioanal. Chem. 416, 1493–1504. https://doi.org/10.1007/s00216-024-05154-7.

Losantos, D., Sarra, M., Caminal, G., 2024b. OPFR removal by white rot fungi: screening of removers and approach to the removal mechanism. Frontiers in Fungal Biology 5, 1387541. https://doi.org/10.3389/ffunb.2024.1387541.

Lu, Q., Lin, N., Cheng, X., Yuan, T., Zhang, Y., Gao, Y., Xia, Y., Ma, Y., Tian, Y., 2022. Simultaneous determination of 16 urinary metabolites of organophosphate flame retardants and organo- phosphate pesticides by solid phase extraction and ultra performance liquid chromatography coupled to tandem mass spectrometry. Chemosphere 300, 134585. https://doi.org/10.1016/j.chemo-sphere.2022.134585.

Luo, K., Liu, J., Wang, Y., Aimuzi, R., Luo, F., Ao, J., Zhang, J., 2020. Associations between organo- phosphate esters and sex hormones among 6–19-year old children and adolescents in NHANES 2013–2014. Environ. Int. 136, 105461. https://doi.org/10.1016/j.envint.2020.105461.

Ma, Z., Tang, S., Su, G., Miao, Y., Liu, H., Xie, Y., Giesy, J.P., Saunders, D.M.V., Hecker, M., Yu, H., 2016. Effects of tris (2-butoxyethyl) phosphate (TBOEP) on endocrine axes during development of early life stages of zebrafish (*Danio rerio*). Chemosphere 144, 1920–1927. https://doi.org/10.1016/j.chemosphere.2015.10.049.

Mir-Tutusaus, J.A., Baccar, R., Caminal, G., Sarrà, M., 2018. Can white-rot fungi be a real wastewater treatment alternative for organic micropollutants removal? A review. Water Res. 138, 137–151. https://doi.org/10.1016/j.watres.2018.02.056.

National Toxicology Program, 2023. NTP Technical Report on the Toxicology and Carcinogenesis Studies of an Isomeric Mixture of Tris(chloropropyl) Phosphate Administered in Feed to Sprague Dawley (HSD: Sprague Dawley® SD®) rats and B6C3F1/N Mice.

Negev, M., Berman, T., Reicher, S., Balan, S., Soehl, A., Goulden, S., Ardi, R., Shammai, Y., Hadar, L., Blum, A., Diamond, M.L., 2018. Regulation of chemicals in children's products: how U.S. and EU regulation impacts small markets. Sci. Total Environ. 616–617, 462–471. https://doi.org/10.1016/j.scitotenv.2017.10.198.

Ning, D., Wang, H., 2012. Involvement of cytochrome P450 in pentachlorophenol transformation in a white rot fungus *Phanerochaete chrysosporium*. PLoS One 7, e45887. https://doi.org/10.1371/journal.pone.0045887.

Pan, H.Y., Cheng, F.J., Huang, K.C., Kung, C. Te, Huang, W.T., You, H.L., Li, S.H., Wang, C.C., Lee, W.C., Hsu, P.C., 2022. Exposure to tris(2-butoxyethyl) phosphate induces abnormal sperm morphology and testicular histopathology in male rats. Ecotoxicol. Environ. Saf. 241, 113718. https://doi.org/10.1016/j.ecoenv.2022.113718.

Petromelidou, S., Evgenidou, E., Lambropoulou, D.A., Petromelidou, S., Evgenidou, E., Lambropoulou, D.A., 2024. Monitoring of OPFRs in WWTPs: unveiling environmental insights with high resolution mass spectrometry. Microchem. J. 205, 111338. https://doi.org/10.1016/j.microc.2024.111338.

Reddy, G.V.B., Gold, M.H., 1999. A two-component tetrachlorohydroquinone reductive dehalo- genase system from the lignin-degrading basidiomycete *Phanerochaete chrysosporium*. Biochem. Biophys. Res. Commun. 257, 901–905. https://doi.org/10.1006/bbrc.1999.0561.

Reddy, G.V.B., Gold, M.H., 2000. Degradation of pentachlorophenol by *Phanerochaete chrysosporium*: intermediates and reactions involved. Microbiology (N Y) 146, 405–413. https://doi.org/10.1099/00221287-146-2-405.

Reddy, G.V.B., Gold, M.H., 2001. Purification and characterization of glutathione conjugate reduc- tase: a component of the tetrachlorohydroquinone reductive dehalogenase system from *Phanerochaete chrysosporium*. Arch. Biochem. Biophys. 391, 271–277. https://doi.org/10.1006/abbi.2001.2417.

Reilly, C.A., Yost, G.S., 2005. Structural and enzymatic parameters that determine alkyl dehydrogenation/hydroxylation of capsaicinoids by cytochrome P450 enzymes. Drug Metab. Dispos. 33, 530–536. https://doi.org/10.1124/dmd.104.001214.

Ren, G., Hu, J., Shang, Y., Zhong, Y., Yu, Z., An, J., 2017. Tributylphosphate (TBP) and tris (2-butoxyethyl) phosphate (TBEP) induced apoptosis and cell cycle arrest in HepG2 cells. Toxicol Res (Camb) 6, 902–911. https://doi.org/10.1039/c7tx00180k.

Romero, S., Blánquez, P., Caminal, G., Font, X., Sarrà, M., Gabarrell, X., Vicent, T., 2006. Different approaches to improving the textile dye degradation capacity of *Trametes versicolor*. Biochem. Eng. J. 31, 42–47. https://doi.org/10.1016/j.bej.2006.05.018.

Sala, B., Giménez, J., de Stephanis, R., Barceló, D., Eljarrat, E., 2019. First determination of high levels of organophosphorus flame retardants and plasticizers in dolphins from Southern European waters. Environ. Res. 172, 289–295. https://doi.org/10.1016/j.envres.2019.02.027.

Saquib, Q., Siddiqui, M., Al-Khedhairy, A., 2021. Organophosphorus flame-retardant tris (1-chloro-2-propyl) phosphate is genotoxic and apoptotic inducer in human umbilical vein endothelial cells. J. Appl. Toxicol. 41, 861–873. https://doi.org/10.1002/jat.4158.

Saquib, Q., Al-Salem, A.M., Siddiqui, M.A., Ansari, S.M., Zhang, X., Al-Khedhairy, A.A., 2022. Tris(2-butoxyethyl) phosphate (TBEP): a flame retardant in solid waste display hepatotoxic and carcinogenic risks for humans. Chemosphere 296, 133977. https://doi.org/10.1016/j.chemosphere.2022.133977.

Sasaki, K., Suzuki, T., Takeda, M., Uchiyama, M., 1984. Metabolism of phosphoric acid triesters by rat liver homogenate. Bull. Environ. Contam. Toxicol. 33, 281–288. https://doi.org/10.1007/BF01625544.

Shi, Y., Gao, L., Li, W., Wang, Y., Liu, J., Cai, Y., 2016. Occurrence, distribution and seasonal variation of organophosphate flame retardants and plasticizers in urban surface water in Beijing, China. Environ. Pollut. 209, 1–10. https://doi.org/10.1016/j.envpol.2015.11.008.

Sutha, J., Anila, P.A., Gayathri, M., Ramesh, M., 2022. Long term exposure to tris (2-chloroethyl) phosphate (TCEP) causes alterations in reproductive hormones, vitellogenin, antioxidant enzymes, and histology of gonads in zebrafish (*Danio rerio*): in vivo and computational analysis. Comparative Biochemistry and Physiology Part - C: Toxicology and Pharmacology 254, 109263. https://doi.org/10.1016/j.cbpc.2021.109263.

Suzuki, T., Sasaki, K., Takeda, M., Uchiyama, M., 1984. Metabolism of tributyl phosphate in male rats. J. Agric. Food Chem. 32, 603–610. https://doi.org/10.1021/jf00123a046.

Takahashi, S., Katanuma, H., Abe, K., Kera, Y., 2017. Identification of alkaline phosphatase genes for utilizing a flame retardant, tris(2-chloroethyl) phosphate, in *Sphingobium* sp. strain TCM1. Appl. Microbiol. Biotechnol. 101, 2153–2162. https://doi.org/10.1007/s00253-016-7991-9.

Tang, B., Xiong, S.M., Zheng, J., Wang, M.H., Cai, F.S., Luo, W.K., Xu, R.F., Yu, Y.J., 2021. Analysis of polybrominated diphenyl ethers, hexabromocyclododecanes, and legacy and emerging phosphorus flame retardants in human hair. Chemosphere 262, 127807. https://doi.org/10.1016/j.chemosphere.2020.127807.

Tayar, S., Losantos, D., Villagra, J., Hu, K., Shokrollahzadeh, S., Sarrà, M., Gaju, N., Martínez-Alonso, M., 2024. Biodegradation of tri-butyl phosphate by *Trametes versicolor* and its application in a trickle bed reactor under non-sterile conditions. Environ. Technol. Innov. 103867. https://doi.org/10.1016/j.eti.2024.103867.

Testa, B., Krämer, S.-D., 2008. The Biochemistry of Drug Metabolism-Volume 1: Principles, Redox Reactions, Hydrolyses. Verlag Helvetica Chimica Acta.

Testa, B., Krämer, S.-D., 2010. The Biochemistry of Drug Metabolism-Volume 2: Conjugations, Consequences of Metabolism, Influencing Factors. Verlag Helvetica Chimica Acta.

Tian, D., Yu, Yihan, Yu, Yingying, Lu, L., Tong, D., Zhang, W., Zhang, X., Shi, W., Liu, G., 2023. Tris(2-chloroethyl) phosphate exerts hepatotoxic impacts on zebrafish by disrupting hypothalamic-pituitary-thyroid and gut-liver axes. Environ. Sci. Technol. 57, 9043–9054. https://doi.org/10.1021/acs.est.3c01631.

Torres-Farradá, G., Thijs, S., Rineau, F., Guerra, G., Vangronsveld, J., 2024. White rot Fungi as tools for the bioremediation of xenobiotics: a review. Journal of Fungi 10, 167. https://doi.org/10.3390/jof10030167.

US Environmental Protection Agency, 2022. Ecological structure activity relationships (ECOSAR) predictive model [WWW document]. URL. https://www.epa.gov/tsca-screening-tools/ecological-structure-activity-relationships-ecosar-predictive-model.
USEPA, 2023. High production volume list [WWW document]. URL. https://comptox.epa.gov/dashboard/chemical-lists/EPAHPV.
Van den Eede, N., Maho, W., Erratico, C., Neels, H., Covaci, A., 2013. First insights in the metabolism of phosphate flame retardants and plasticizers using human liver fractions. Toxicol. Lett. 223, 9–15. https://doi.org/10.1016/j.toxlet.2013.08.012.
Van den Eede, N., Erratico, C., Exarchou, V., Maho, W., Neels, H., Covaci, A., 2015. In vitro biotrans- formation of tris(2-butoxyethyl) phosphate (TBOEP) in human liver and serum. Toxicol. Appl. Pharmacol. 284, 246–253. https://doi.org/10.1016/j.taap.2015.01.021.
Van den Eede, N., de Meester, I., Maho, W., Neels, H., Covaci, A., 2016a. Biotransformation of three phosphate flame retardants and plasticizers in primary human hepatocytes: untargeted metabolite screening and quantitative assessment. J. Appl. Toxicol. 36, 1401–1408. https://doi.org/10.1002/jat.3293.
Van den Eede, N., Tomy, G., Tao, F., Halldorson, T., Harrad, S., Neels, H., Covaci, A., 2016b. Kinetics of tris (1-chloro-2-propyl) phosphate (TCIPP) metabolism in human liver microsomes and serum. Chemosphere 144, 1299–1305. https://doi.org/10.1016/j.chemosphere.2015.09.049.
Vijay, G., Reddy, B., Sollewijn Gelpke, M.D., Gold, M.H., 1998. Degradation of 2,4,6-trichlorophenol by *Phanerochaete chrysosporium*: involvement of reductive dechlorination. J. Bacteriol. 180, 5159–5164.
Wang, G., Chen, H., Du, Z., Li, J., Wang, Z., Gao, S., 2017. In vivo metabolism of organophosphate flame retardants and distribution of their main metabolites in adult zebrafish. Sci. Total Environ. 590–591, 50–59. https://doi.org/10.1016/j.scitotenv.2017.03.038.
Wang, X., Zhong, W., Xiao, B., Liu, Q., Yang, L., Covaci, A., Zhu, L., 2019. Bioavailability and bio-magnification of organophosphate esters in the food web of Taihu Lake, China: impacts of chemical properties and metabolism. Environ. Int. 125, 25–32. https://doi.org/10.1016/j.envint.2019.01.018.
Wang, H., Jing, C., Peng, H., Liu, S., Zhao, H., Zhang, W., Chen, X., Hu, F., 2022. Parental whole life-cycle exposure to tris (2-chloroethyl) phosphate (TCEP) disrupts embryonic development and thyroid system in zebrafish offspring. Ecotoxicol. Environ. Saf. 248, 114313. https://doi.org/10.1016/j.ecoenv.2022.114313.
Wei, B., O'Connor, R., Goniewicz, M., Hyland, A., 2020. Association between urinary metabolite levels of organophosphorus flame retardants and serum sex hormone levels measured in a reference sample of the US general population. Expo. Health 12, 905–916. https://doi.org/10.1007/s12403-020-00353-w.
Winder, C., Azzi, R., Wagner, D., 2005. The development of the globally harmonized system (GHS) of classification and labelling of hazardous chemicals. J. Hazard. Mater. 125, 29–44. https://doi.org/10.1016/j.jhazmat.2005.05.035.
Wong, S.H., Bell, S.G., De Voss, J.J., 2017. P450 catalysed dehydrogenation. Pure Appl. Chem. 89, 841–852. https://doi.org/10.1515/pac-2016-1216.
Wu, Y., Su, G., Tang, S., Liu, W., Ma, Z., Zheng, X., Liu, H., Yu, H., 2017. The combination of in silico and in vivo approaches for the investigation of disrupting effects of tris (2-chloroethyl) phosphate (TCEP) toward core receptors of zebrafish. Chemosphere 168, 122–130. https://doi.org/10.1016/j.chemosphere.2016.10.038.
Xiong, H., Huang, Y., Mao, Y., Liu, C., Wang, J., 2021. Inhibition in growth and cardiotoxicity of tris (2-butoxyethyl) phosphate through down-regulating Wnt signaling pathway in early develop- mental stage of zebrafish (*Danio rerio*). Ecotoxicol. Environ. Saf. 208, 111431. https://doi.org/10.1016/j.ecoenv.2020.111431.
Xiong, Y., Shi, Q., Smith, A., Schlenk, D., Gan, J., 2023. Methylation and demethylation of emerging contaminants changed bioaccumulation and acute toxicity in *Daphnia magna*. Environ. Sci. Technol. 57, 15213–15222. https://doi.org/10.1021/acs.est.3c03242.
Xiong, Y., Shi, Q., Li, J., Sy, N.D., Schlenk, D., Gan, J., 2024. Methylation and demethylation of emerging contaminants in plants. Environ. Sci. Technol. 58, 1998–2006. https://doi.org/10.1021/acs.est.3c03171.
Xu, T., Li, P., Wu, S., Lei, L., He, D., 2017a. Tris(2-chloroethyl) phosphate (TCEP) and tris (2-chloro- propyl) phosphate (TCPP) induce locomotor deficits and dopaminergic degeneration in *Caenorhabditis elegans*. Toxicol Res (Camb) 6, 63–72. https://doi.org/10.1039/c6tx00306k.
Xu, Q., Wu, D., Dang, Y., Yu, L., Liu, C., Wang, J., 2017b. Reproduction impairment and endocrine disruption in adult zebrafish (*Danio rerio*) after waterborne exposure to TBOEP. Aquat. Toxicol. 182, 163–171. https://doi.org/10.1016/j.aquatox.2016.11.019.
Xu, L., Hu, Q., Liu, J., Liu, S., Liu, C., Deng, Q., Zeng, X., Yu, Z., 2019. Occurrence of organophosphate esters and their diesters degradation products in industrial wastewater treatment plants in China: implication for the usage and potential degradation during production processing. Environ. Pollut. 250, 559–566. https://doi.org/10.1016/j.envpol.2019.04.058.
Yan, J., Zhao, Z., Xia, M., Chen, S., Wan, X., He, A., Daniel Sheng, G., Wang, X., Qian, Q., Wang, H., 2022. Induction of lipid metabolism dysfunction, oxidative stress and inflammation response by tris(1-chloro-2-propyl)phosphate in larval/adult zebrafish. Environ. Int. 160, 107081. https://doi.org/10.1016/j.envint.2022.107081.
Yang, J., Li, Q., Li, Y., 2020. Enhanced biodegradation/photodegradation of organophosphorus fire retardant using an integrated method of modified pharmacophore model with molecular dynamics and polarizable continuum model. Polymers (Basel) 12, 1672. https://doi.org/10.3390/POLYM-12081672.
Yang, D., Wei, X., Zhang, Z., Chen, X., Zhu, R., Oh, Y., Gu, N., 2022. Tris (2-chloroethyl) phosphate (TCEP) induces obesity and hepatic steatosis via FXR-mediated lipid accumulation in mice: long-term exposure as a potential risk for metabolic diseases. Chem. Biol. Interact. 363, 110027. https://doi.org/10.1016/j.cbi.2022.110027.
Yao, C., Li, Y., Li, J., Jiang, C., Jing, K., Zhang, S., Yang, H., Liu, C., Zhao, L., 2023. Aerobic degradation of parent triisobutyl phosphate and its metabolite diisobutyl phosphate in activated sludge: degradation pathways and degrading bacteria. J. Hazard. Mater. 460, 132380. https://doi.org/10.1016/j.jhazmat.2023.132380.
Yu, X., Yin, H., Ye, J.S., Peng, H., Lu, G., Dang, Z., 2019. Degradation of tris-(2-chloroisopropyl) phosphate via UV/TiO_2 photocatalysis: kinetic, pathway, and security risk assessment of degradation intermediates using proteomic analyses. Chem. Eng. J. 374, 263–273. https://doi.org/10.1016/j.cej.2019.05.193.
Zhang, Q., Wang, J., Zhu, J., Liu, J., Zhao, M., 2017. Potential glucocorticoid and mineralocorticoid effects of nine organophosphate flame retardants. Environ. Sci. Technol. 51, 5803–5810. https://doi.org/10.1021/acs.est.7b01237.
Zhang, Q., Yu, C., Fu, L., Gu, S., Wang, C., 2020a. New insights in the endocrine disrupting effects of three primary metabolites of organophosphate flame retardants. Environ. Sci. Technol. 54, 4465–4474. https://doi.org/10.1021/acs.est.9b07874.
Zhang, R., Yu, K., Li, A., Zeng, W., Lin, T., Wang, Y., 2020b. Occurrence, phase distribution, and bioaccumulation of organophosphate esters (OPEs) in mariculture farms of the Beibu Gulf, China: a health risk assessment through seafood consumption. Environ. Pollut. 263, 114426. https://doi.org/10.1016/j.envpol.2020.114426.
Zhang, S., Li, Y., Yang, C., Meng, X.Z., Zheng, H., Gao, Y., Cai, M., 2021a. Application of Hi-throat/Hi-volume SPE technique in analyzing occurrence, influencing factors and human health risk of organophosphate esters (OPEs) in drinking water of China. J. Environ. Manag. 291, 112714. https://doi.org/10.1016/j.jenvman.2021.112714.
Zhang, H., Liu, T., Song, X., Zhou, Q., Tang, J., Sun, Q., Pu, Y., Yin, L., Zhang, J., 2021b. Study on the reproductive toxicity and mechanism of tri-n-butyl phosphate (TnBP) in *Caenorhabditis elegans*. Ecotoxicol. Environ. Saf. 227, 112896. https://doi.org/10.1016/j.ecoenv.2021.112896.
Zhang, X., Bi, Y., Fu, M., Zhang, Xinyu, Lei, B., Huang, X., Zhao, Z., 2023a. Organophosphate tri- and diesters in source water supply and drinking water treatment systems of a metropolitan city in China. Environ. Geochem. Health 45, 2401–2414. https://doi.org/10.1007/s10653-022-01333-6.
Zhang, Y., Cui, W., Zhang, N., Qin, P., Zhang, Ying, Guo, X., Wang, Z., Lu, S., 2023b. Occurrence and risk of organophosphate flame retardants in multiple urban water of Beijing, China. Water Air Soil Pollut. 234, 1–10. https://doi.org/10.1007/s11270-023-06277-w.
Zhang, Q., Wang, Y., Lou, J., Ying, Z., Mo, X., Lin, S., 2024. Infant exposure and risk assessment of organophosphorus flame retardants in human breast milk from the Southeast City, China. Expo. Health 16, 279–289. https://doi.org/10.1007/s12403-023-00552-1.
Zhao, Y., Fan, Y., Li, J., Liu, Y., Lv, Y., Zhao, L., Hou, G., An, Z., Cai, W., Li, X., Wu, W., Cao, Z., 2023. Assessment of human exposure to traditional and novel organophosphate esters via multiple personal matrices. Environ. Sci. Technol. 58, 3332–3341. https://doi.org/10.1021/acs.est.3c07282.
Zheng, G., Schreder, E., Dempsey, J.C., Uding, N., Chu, V., Andres, G., Sathyanarayana, S., Salamova, A., 2021. Organophosphate esters and their metabolites in breast milk from the United States: breastfeeding is an important exposure pathway for infants. Environ. Sci. Technol. Lett. 8, 224–230. https://doi.org/10.1021/acs.estlett.0c00916.
Zhuo, R., Fan, F., 2021. A comprehensive insight into the application of white rot fungi and their lignocellulolytic enzymes in the removal of organic pollutants. Sci. Total Environ. 778, 146132. https://doi.org/10.1016/j.scitotenv.2021.146132.